Experimental Investigations on the Mechanical Properties of a Disc Fabricated from AA5052 Wastes through Friction Stir Consolidation Process

A thesis submitted by

Samuel Kefyalew

For the Partial fulfilment of the

Requirement for the award of degree

Of

Master of Science

In Manufacturing Engineering

Under the Supervision & Guidance of

Dr. Desalegn Wogaso (PhD)

Assistant Professor

Mechanical Design & Manufacturing Engineering Program

School of Mechanical, Chemical and Materials Engineering

Adama Science and Technology University

Adama, Ethiopia

June 2018

Mechanical Design and Manufacturing Engineering Program

Adama, Ethiopia

Experimental Investigation on the Mechanical Properties of a Disc Fabricated from AA5052 Wastes through Friction Stir Consolidation Process

By

Samuel Kefyalew Abebe

Approved by Board of Examines

Chair, department graduate committee	Signature	Date
______________________________	________	____________
Advisor	Signature	Date
______________________________	________	____________
Internal examiner	Signature	Date
______________________________	________	____________
External examiner	Signature	Date
______________________________	________	____________

CANDIDATE DECLARATION

I hereby declare that the work which is being presented in this thesis entitled **"Experimental Investigation on the Mechanical Properties of a Disc Fabricated from AA5052 Wastes through Friction Stir Consolidation Process".** In partial fulfilment of the requirement for the award of the degree of Masters of Science in Manufacturing Engineering is my own work carried out **September to June 2018** under the supervision of **Dr. Desalegn Wogaso**, program of Mechanical Design and Manufacturing Engineering, Adama Science and Technology University, Adama, Ethiopia.

The matter embodied in this thesis has not been submitted by me for the award of any other degree or diploma. All relevant resources of information used in this thesis have been duly acknowledged.

Samuel Kefyalew Abebe ______________ ______________

Candidate Signature Date

This is to certify that the above declaration made by the candidate is correct to the best of my knowledge and belief. This thesis has been submitted for examination with my approval.

Dr. Desalegn Wogaso (PhD) ______________ ______________

Advisor Signature Date

ACKNOWLEDGEMENT

Next to the almighty God, this thesis was made possible due to the masterly guidance of Dr. Desalegn Wogaso. I was nourished profoundly from your erudite knowledge, dedication to work and spirit of always seek truth from facts. You set a good example of both experimentalist and researcher. Those countless brainstorm helps me to think critically and deeply, today and tomorrow. Your advices and methodology are still guiding me find the right path. I thank you very much that you gave me a perfect advices whenever I faced a serious problems and you made me feel hopeful to finish this thesis.

To make my past two years unique, not only it is a course of pursuing master degree but also a wonderful journey of knowing friends come from all over the country. I am amazed by the transcultural communications between people who born in different area of the country and cultures apart, who exchange thoughts with spark but respects as well. I sincerely thank all my friends: Naol Desalegn, Worku Mamuye, Gizaw Yohannes and special thanks to Mr. Mengistu Gelaw who help me from the very beginning to the end, and many people who worked with me and help me in academic area or daily life. All little drops of time shared with you come together as a priceless stream that will always flow in my mind.

I also gratitude to Mr. Abdulmelik Hasen, Head of Mechanical Design and Manufacturing Engineering for his continuous help and to Senayit Alemayehu, shop keeper of program of Mechanical Design and Manufacturing Engineering, Kamil husen, laboratory technician, Material Science and Engineering Department for his technical support during mechanical property testing of samples. Finally I would like to thank Dr. Habtamu Beri, Dean, School of Mechanical, Chemical and Materials Engineering, Adama Science and Technology University. For his administrative support in the work.

ABSTRACT

Friction stir consolidation (FSC) is a recently developed metal working technology which involves a solid-phase manufacturing process that consolidates metal powder, chips or scraps into solid blocks via severe plastic deformation and solid state welding. It has the capability to be a more economical and "green" process to recycle metal waste. The objective of this research was to experimentally investigate and optimize the process parameters of friction stir consolidated solid disc fabricated from AA5052 wastes and finding enhanced mechanical properties namely compression strength and hardness. In this research, solid discs were produced from AA5052 aluminum alloy machining wastes through friction stir consolidation process. Furthermore, design of experiment was conducted to quantify and optimize the effect of die rotational speed, aspect ratio and processing time on compression strength and hardness. Likewise experiments were conducted by taking three factors and three levels namely: speed (315 rpm, 400 rpm and 500 rpm), aspect ratio (25.4/7, 25.4/5 and 25.4/3) and time (30s, 45s and 60s) then compression strength and hardness were determined and optimized. MINITAB 2017 software was used to identify the optimum input factors with their corresponding levels. L9 orthogonal array was used and for each set up three trials were taken to reduce variability occurred due to noise factors. Results show that for both compression strength and hardness, the optimum processing condition is: a process with speed, aspect ratio and time set at levels of 500 rpm, 25.4/3 and 60s respectively. Verification experiment was carried out for the response of hardness and compression strength. The result shows that experimentation was consistent and the obtained results are reliable. The main effect plot for signal to noise ratio revealed that aspect ratio and time have a great influence on the responses. For compression strength the percentage contribution of aspect ratio, Speed and Time were analyzed as 77.69%, 5.32% and 4.27% respectively with error of 12.72%. Furthermore for hardness MINITAB 17 predicted the percentage contribution of Aspect ratio, Speed and Time were 88.33%, 3.63% and 7.61% respectively with error of 0.43%.

Key words**:** *Friction stir consolidation, Microstructure, Design of experiment, Hardness and Compression strength.*

TABLE OF CONTENTS

LIST OF TABLES

LIST OF FIGURES

ABRIVIATIONS AND ACRONYMS

A	Area
AA	Aluminum Alloy
ANOVA	Analysis of Variance
ASTM	American Society for Testing Materials
D	Cutter Diameter
D_2	High performance hot working tool
DOE	Design of Experiment
E	Experiment
ECAP	Equal Channel Angular Pressing
EDM	Electric Discharge Machine
FEA	Finite Element Analysis
FEP	Friction Extrusion Process
FSC	Friction Stir Consolidation
FSCP	Friction Stir Consolidation Process
FSP	Friction Stir Process
FSW	Friction Stir Welding
GHG	Green House Gas
HB	Brinell Hardness
HV	Vickers Hardness
iECAP	integrated Equal channel Angular Press
LB	Lower is better
N	Rotational speed of cutter
n	number of teeth
NB	Nominal is best
OA	Orthogonal array
PDS	Process Development System
Rpm	Revolution per minute
S/N	Signal to Noise ratio
SEM	Scanning Electron Microscope

SPD	Severe Plastic Deformation
SD	Standard Deviation
t_c	Chip thickness
v	Linear speed
W	Weight

CHAPTER ONE: BACKGROUND OF THE STUDY

1.1 Introduction

Friction stir processing is the new and promising thermomechanical processing method that adjusts the mechanical properties and microstructure of the material in single pass to attain maximum performance with less manufacturing cost in less time using cheaper and simple tool. Friction stir consolidation is a solid-state processing technique that uses a non-consumable rotating die to create frictional heat and plastic deformation resulting in particulate bonding and microstructural modification. Originally it was developed for processing of aluminum and magnesium based structural alloys because of their lower melting point and high application.

Aluminum and its alloys have got much attention as important materials in construction, automobile, and aerospace industries because of their high strength-to-weight ratio and good formability. They are preferable because of their excellent physical properties such as high specific strength, low density, high specific stiffness, high thermal conductivity, and good manufacturability for machining and casting. Manufacturing operations, especially traditional machining, usually produce considerable amounts of aluminum waste in the form of scraps.

There are two primary techniques of recycling of non-ferrous metals (i.e. aluminum and its alloys) chips to attain a useful product: the so-called 'conventional' technique and the direct conversion technique (Tekkaya *et al*. (2009), (Tang and Reynolds, (2010)). The conventional method needs melting of the material to be recycled, casting of a billet, and hot extrusion of the billet to form the final product in wire or rod form. Direct recycling of aluminum chips via hot extrusion was first proposed and patented by (Stern (1945)). Gronostajski and Matuszak (1999) broke down and compacted aluminum chips followed by conventional hot extrusion process. This solid state process eliminates creation of thick oxide skin so that the scrap can be changed to a final product without requiring additional processing. The direct conversion method uses conventional hot extrusion which may or may not be preceded by a static pressing stage. Compared with conventional recycling, the direct conversion of aluminum scrap into compact metal may result in 26–31% energy, 40% material, and 16–60% labor savings (Gronostajski *et al.* (2000)). The benefit of direct or solid phase recycling of aluminum are perceived to be important by researchers. It can minimize cost of energy consumption and environmental protection as compared to the conventional recycling. In addition, significant amount of carbon footprint also can be cut down. In secondary aluminum production, energy about 10 GJ/ton of the material is required, comprises about 5-10 % of the energy in the primary aluminum output, and the trend is growing for the subsequent years. In 2030, a recycling rate of 50% is expected (Shamsudin *et al.* (2016)). The percentage figures shows that demand for energy in secondary aluminum processing through re-melting is increased significantly. Although there have been several perfect efforts to improve energy efficiency of melting furnaces since the 1980s, however, the energy requirement for secondary aluminum production can still go up to 20 GJ/ton depending on the way of production facilities, aluminum scrap and processes (Shamsudin *et al.* (2016)). In the case for aluminum chips, the conventional recycling technique or method was unfavorable due to a significant metal loss. Low density of the compacted chips enhances losses through oxidation. There are further losses on each stage of subsequent processing caused ultimately no more than 54% of the metal is regained during conventional recycling by melting (Shamsudin *et al.* (2016)). For instance, conventional recycling of aluminum turnings caused to approximately 45% losses in the metal (Shamsudin *et al.* (2016)). The losses influenced to cost rising in labor, expenditures and energy for environmental protection which subsequently raises the total cost of the process. The direct recycling of aluminum is lesser in steps involved, suitability of improving material properties to the better extent and higher recovery efficiency (Shamsudin *et al.* (2016)).

Friction stir welding (FSW) and Friction stir processing (FSP) are solid phase or solid state processes for joining and microstructure modification, respectively. Both of them depend on plastic dissipation for heat creation or generation and may be taken as severe plastic deformation processes (SPD). FSW was patented by The Welding Institute (UK) in 1991 (Thomas *et al.* (1991)). In both technologies, a rotating non-consumable tool, processing and welding, is used to generate a plasticized surface which undergoes heating and severe plastic deformation. In general, friction stir processing results in finer grains in the processed zone due to the application of temperature and sever plastic deformation.

1.2 Aluminum Alloy 5052

Typical applications of aluminum 5052 alloy include aircraft, marine, architecture, heat exchangers, general sheet metal work, fuel lines and tanks, flooring panels, appliances, streetlights, rivets, washers and can be input for another processes to produce different machine parts. The high corrosion resistance of AA5052 alloy against salt spray and seawater makes it a main candidate for the failure-sensitive structures of large marines, like tanks of liquefied natural gas tankers. The material composition of AA5052 is shown in Table 1.1 below.

Table 1.1 Composition (Wt. %) of AA5052 alloy (Oberg *et al.* (2008)).

Magnesium	Chromium	Copper	Iron	Manganese	Silicon	Zinc
2.2-2.8	0.15-0.35	0.1 max.	0.4 max.	0.1 max.	0.25 max.	0.1 max.

1.3 Statement of the Problem

During the production of aluminium components, much of the original material is rejected as waste, e.g. swarf, metal chips, etc. Low density of the compacted chips increases losses through oxidation. In addition, losses on each stage of subsequent processing causes ultimately not more than 54% of the metal is recovered during conventional recycling by means of melting. The conventional recycling method is unfavourable due to a significant metal loss. Ultimately, it is desired to establish a manufacturing process which involves more percentage of recovery and lesser process steps. Manufacturing methods like casting, forming and machining can manufacture a fully consolidated disc but they require multi-step processing time. However, through FSC process, manufacturing can be done with minimum number of steps. It is preferable due to its environmentally friendliness, minimum defects and wastages are observed. The defects in a casting process like shrinkage, gas porosity, and other metallurgical defects can be highly minimized by using an alternative FSC process.

1.4 Research Questions

The research questions were:

1) What clamping system was needed to run the experiment?
2) Was the FSC feasible process to recycle aluminum wastes?
3) How to collect the experimental data?
4) How did the mechanical properties of a disk obtained?
5) What was the effect of process parameters on the mechanical properties of the consolidate disc (strength and hardness)

6) How to conclude and decide the optimum mechanical properties (hardness and compression strength)?
7) What were the effect of process parameters (like aspect ratio, speed and time) on hardness and compressive strength of the disk?

1.5 Objectives of the Research

1.5.1 General Objective

The objective of this research was to experimentally investigate and optimize the process parameters of friction stir consolidated solid disc from AA5052 wastes thereby obtain enhanced mechanical properties particularly compression strength and hardness.

1.5.2 Specific Objectives

- To design (geometrical design) jigs, fixtures and dies set up for FSC process on a milling machine.
- To manufacture jigs, fixtures and dies set up for FSC process on a milling machine.
- To determine the mechanical properties (compression strength and hardness) through appropriate mechanical testing.
- To conduct an experiment to manufacture AA5052 disk for different experimental condition.
- To investigate the optimum input factors for the enhanced mechanical property namely compression strength and hardness using design of experiment.
- To investigate the microstructures for the mechanical property optimized disk.
- To re-manufacture a disc with the obtained optimum input factors and re-testing for verification.

1.6 Significance of the Research

The outcome of the research can be used as:

- Input for all aluminum and its alloy processing industries.
- Highly reduced amount of environmental pollution and near zero emission of CO_2, metal oxide particulate and elimination of greenhouse gas (GHG) emissions.
- To minimize processing steps.
- Potential for metal recycling with much less energy compared to conventional process.

- To reduce defects as compared to casting.
- To reduce labor cost as a result the processing steps can be minimized.

1.7 Scope and Limitation of the Research

This study was limited to geometrical design and manufacture of dies and fixture set up to process AA5052 disk on a milling machine from AA5052 waste. Additionally, conducting design of experiment in investigating the effects of input process parameters (aspect ratio, consolidating time and die rotational speed) on the mechanical properties of the disc namely compression strength and hardness.

During the experimentation of FSC process, there were three major problems that were observed frequently. The first problem was the uncontrollable vibration of the existing milling machine (i.e. milling machine model FU 281) and it was resulted in creating high disturbing sound and heating of dies before the consolidation had occurred. To reduce the heating of dies, it was required to increase the clearance between the rotating die and a stationary chamber to 0.2 mm which was previously 0.02 mm. And this problem resulted in the formation of flashes at the edge of the produced discs. This was the cause for the second problem to occur. The second problem was weldment of rotating die with a stationary chamber due to the plasticized aluminum flow through the gap or through the maximized clearance between them. The maximum power of the existing machine (i.e. milling FU281) was only 5.5 KW which stops while the plasticized aluminum flows through the clearance. This was one of the most commonly observed problem that had faced during experimentation. Thirdly, the removal of the produced disc was another problem faced in this research in which the chamber needs to be split rather than enclosed or cylindrical for easy removal of the discs. Unavailability of functional EDM machine resulted in using enclosed cylindrical chamber. In addition to this the consequence of the unavailability of the proper chemicals for etchants and SEM machine resulted in a blurred image of microstructure or grain boundaries. Which resulted in difficulty of grain size determination. These were the major problems which had observed during experimentation without mentioning the bureaucratic problem of some offices and financial shortage.

1.8 Thesis Organization

This thesis consists of five chapters:

Chapter one describes a general introduction of the friction stir processes and aluminum alloy. Chapter two presents literature review about the friction stir consolidation, friction stir processing and Taguchi`s optimization technique. Chapter three describes materials and methods which were used to design and fabricate dies, chips preparation, experimental procedure and optimization of the mechanical properties of produced disk and sample preparation method for the testing. Chapter four presents about results and discussions. Finally, chapter five presents conclusion and recommendation of the current research work and future scope of the work.

CHAPTER TWO: LITERATURE REVIEW

2.1 General Background

Friction stir consolidation was invented at the Welding Institute (Cambridge UK) in the early 1990`s. After that it was basically disregarded for years until early 2010`s. The growth of additive manufacturing and aerospace industry awaken attention to friction stir consolidation and extrusion processes due to they have great capability in recycling.

2.2 Direct Recycling of Aluminum Wastes

Recycling of metal reduces the consumption of fresh material and prevents pollution and waste. Recycling aluminum can save up to 95% of the energy that would be needed to create a comparable amount from raw material. Avenues to recycle aluminum wastes can be classified into two categories: one is the conventional method which involves re-melting, the other is the direct method without re-melting (Tekkaya *et al.* (2009)). Process for conventional methods of recycling and reuse consist of multiple steps of refining re-melting and casting, which are complex and require considerable labor and power (Gronostajski and Matuszak (1999)). Special devices and strict working environment are needed due to high temperature and liquid state metal involved. In 1945, stern first proposed and patented hot extrusion as a direct recycling process (Stern Max (1945)). Sharma *et al.* (1977) produced aluminum bar and aluminum cans from aluminum swarf via hot extrusion and back can extrusion, respectively. The success of these methods indicates that high temperatures, high deformation, and high pressure play critical roles in solid phase metal recycling.

Over the past 20 years, there was additional work on developing direct recycling convert aluminum chips into a final product (Gronostajski *et al.* (1997)). The post process analysis indicated that high density and good properties can be achieved when sufficient extrusion pressure and temperature were utilized. Galanty (2000) showed that room temperature extrusion can be adopted to consolidate aluminum chips into a high density extrudate. Tekkaya *et al.* (2009) pointed out that the keys to recycling aluminum chips via hot extrusion are high pressure, temperature and strain level inside the die. Misiolek *et al.* (2012) discussed traditional compaction, multi-layer compaction, and the front-pad approach for powder extrusion.

Three types of die: flat-face die, porthole die, and equal channel angular pressing (ECAP), have been compared. The result showed that use of ECAP leads to sufficient bonding and higher ductility the extrudate compared to other methods. Wideroe and Welo (2013) implemented screw extrusion as a new route to recycle aluminum chips. This process combines compaction and extrusion in a single step by generating frictional heat and plastic dissipation of work.

Paraskevas (2014) proposed spark plasma sintering (SPS) as a novel solid phase recycling technique. However, the surface oxides of aluminum chips are not totally fractured hence the inter-chip bonding is weaker than the parent metal. By extensive literature review, (Cooper and Allwood (2014)) established a film theory of bonding to derive a model that quantifies the relevant deformation parameters relating to weld strength between chips The experimental result shows a minimum strain is required for good bonding. The value of the required minimum strain is related to temperature and normal contact stress or shear stress. Duflou *et al.* (2015) compared several aluminum recycling methods and assessed their environment impact. The screw extrusion was found to have the lowest environment impact contribution due to its low metal loss percentage (solid state process) and high energy efficiency (fewer heating-cooling steps).

Quantification of deformation status in friction extrusion has not been published, but there is some other related work in the literature. Direct recycling of aluminum chips via hot extrusion was first proposed and patented by (Stern (1945)). Gronostajski and Matusza (1999) comminuted and compacted aluminum chips succeeded by conventional hot extrusion. This solid state process avoids the formation of thick oxide skin so the scrap can be transformed to a final product without requiring further processing. The process was also used for the growth of new alloy compositions on the basis of blending or mixing of multiple alloy particulates.

A recent study indicates that improved performance extrudates can be fabricated when proper die design criteria are fulfilled (Misiolek *et al*. (2012)). Tekkaya *et. al*. (2009) showed that the pre-compaction step is not important when minimum temperature strain and stress conditions are obtained in order to create metallic bonding among chips. Haase *et al.* (2012) use the integrated equal channel angular pressing (iECAP) die rather than the porthole die or the flat-face as a tool for solid state recycling of aluminum machining chips. Since additional strain and shear deformation are introduced, improved strength, superior chip bonding and ductility are achieved. McDonald *et al.* (2014) also used ECAP to recycle Ti-6Al- 4V machining chips to fabricate fully dense material. Compared with commercial Ti-6Al-4V, improved mechanical properties are obtained after mill-annealing treatment. Güley *et al*. (2013) identified the welding performance and quality of using flat-face die and porthole die via numerical simulation and conducting experiments. The bonding criteria of chips and the breakdown mechanism of oxide layer were formed. The welding quality index (WQI) related to effective stress and normal pressure has been proposed. Cooper and Allwood (2014) Reviewed previous experimental and theoretical work on solid bonding. The summation of experiments showed that a less strain is needed for bonding. Increasing the normal contact stress or shear stress, temperature can reduce this required minimum strain. A normal contact stress above the materials' uniaxial yield stress is necessary to generate a strong bond. Haase and Tekkaya (2015) further processed hot extruded chips by forward rod extrusion or backward can extrusion. By comparing the result of mechanical tests and microstructure, it was shown that the deformation route during hot extrusion is critical to improved quality of final products.

Duflou *et al*. (2015) studied the significant environmental impact minimization related to solid state recycling processes. 4% less material loss were recorded for screw extrusion when considering average industrial material loss fraction. Using a similar principle to that of friction extrusion, a testing machine using combined shear and pressure to granulate and recycle aluminum was built by (Widerøe *et al*. (2010)). Their results showed that the shear deformation is highly minimized the axial force needed for compacting aluminum scrap. Also, they indicated that the number of revolutions of the tool affects deformation penetration depth and mixing range. Since limited experimental parameters were used, the relationships between process responses control parameters and such as microstructure and material flow pattern were not determined.

Widerøe and Welo (2013) observed spiral core path as a possible material flow path in screw extrusion. Their result indicates that the highest rate of material flow was found in the center of screw channel and dead metal zones were located at the bottom of the screw channel and toward the container wall. The above studies indicate that extrusion at high temperature is not only an economical avenue to recycle aluminum chips. However, it is also a base to fabricate high quality finished products. Relative to traditional hot extrusion, friction extrusion needs considerably less extrusion force to produce high strain and deformation.

2.3 Friction Stir Processing and Consolidation

A friction forging process was developed in 1975 by Gilpin and Andrews (1975). They described the use of a die in a friction welding process to shape the resultant flash but it is not related with extrusion. Next to this process, the friction extrusion process (FEP) was invented and patented in early 1990s by W. Thomas (Thomas *et al.* (1993)). However, the friction extrusion process lay dormant for several years. Recently, FEP was adopted as a friction-based extrusion method for producing high quality wire or rod from low-cost precursors (e.g., powders and chips) (Tang and Reynolds (2010)). The potential of using friction stir processed material as feedstock in additive manufacturing was proven (Li *et al.* (2015)). The material flow in the extruded wire (Li *et al.* (2013)) and the consolidated disc (Li *et al.* (2012)) were visualized and discussed with different tool tip patterns and experimental parameters. The strain and crystallographic texture of friction extruded wire were studied (Li *et al.* (2016)). However, neither the consolidated disc nor the consolidation process in FEP was analyzed.

Friction stir consolidation, FSC, a similar technology to FEP, was developed as a potential recycling process for processing of metals and alloys and proposed as a convenient manufacturing process for producing high quality metallic products from finely divided precursors or metal wastes in one step with relatively simple equipment requirements (Tang and Reynolds (2011)).

The principle of FSC is shown in Figure 2.1. A cylindrical die with rotating motion is pressed onto finely divided metals or alloys which is confined in a billet chamber. The heat generated by friction and plastic deformation results in softening of the material. Undergoing rotation and compression, the interparticle gaps are diminished and then the softened particles are welded together and consolidated. Therefore these finely divided materials are fully compacted into a solid block. Low porosity (Catalini *et al.* (2013)) and refined grain structure (Whalen *et al.* (2016)) have been achieved via FSC to produce oxide dispersion strengthened material (Catalini *et al.* (2015)) and thermoelectric material (Catalini *et al.* (2013)).

As a direct method to recycle metal chips or scraps, FSC may be considered as more economical and "green" process when compared with conventional recycling process involving melting and casting. Since it is a single step process, much time, labor, and material may be saved from replacing the multi-step recycling process.

2.4 Principle of Friction Stir Consolidation Process

Principle of friction stir consolidation is a method of manufacturing which uses compressive force and torque to create a frictional heat to melt the work. The following Figure 2.1 shows the arrangement of the rotating die, backing plate and chamber.

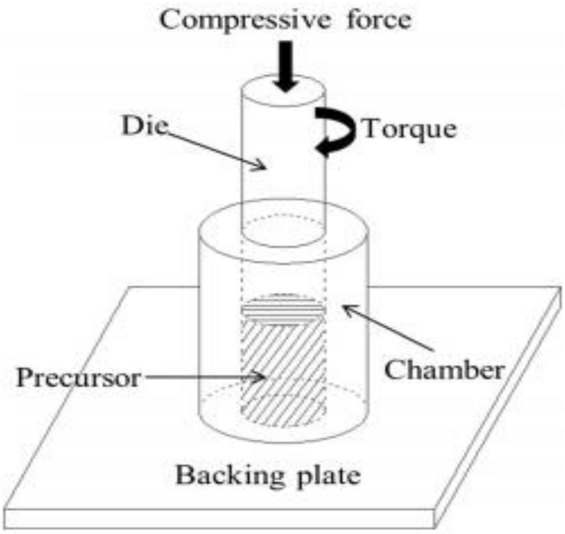

Figure 2. 1 Principle of FSC (Li1 *et al*. (2017))

Due to the compressive force and rotational effect of the rotating die, heat will be occurred inside the chamber then the produced heat will result in plasticizing of the precursor. Backing plate and chamber holds the precursors and exposes them for the rotating die. The compressive force is used to increase the friction. Then due to the heat produced as a result of frictional force, the weldment or consolidation among chips or precursors will be occurred.

2.5 Factors Affecting Friction Stir Consolidation

The process parameters for friction stir extrusion are broadly classified into three groups: (a) tooling related parameters: linear velocity; (b) machine related parameters: plunge force or depth, spindle speed, axial force rate, etc. and (c) die related parameters: die material, texture of die and tool, size of the die etc. The influencing process parameters are illustrated using a cause-effect diagram.

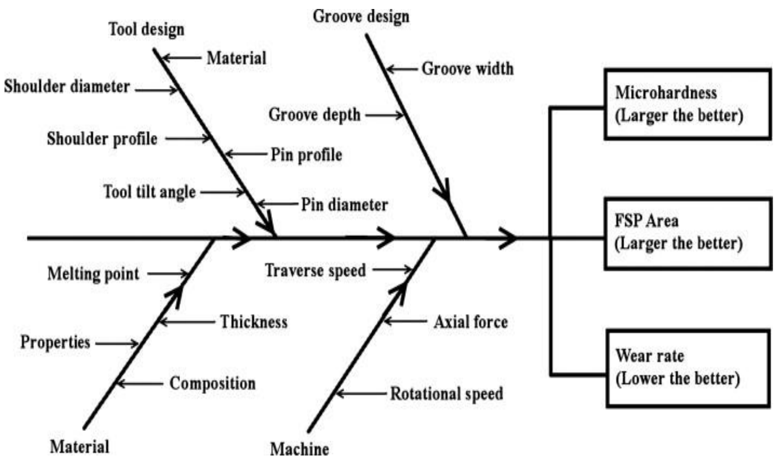

Figure 2. 2 Factors affecting FSP (Sathiskumar *et al.* (2013))

2.6 Conventional Manufacturing Method Related to Friction Stir Consolidation Process

In this section, Conventional Manufacturing Method Related to Friction Stir Consolidation Process are reviewed and discussed. Their advantages and disadvantages are also elaborated. Comparison of several manufacturing process related to FSC are conducted.

2.6.1 Powder Metallurgy

Powder metallurgy is a process of producing useful components parts from metal powders by pressing and simultaneous or subsequent heating to produce a coherent mass. The conventional powder metallurgy process consists of three operations: powder blending and mixing, powder pressing, and compact sintering. Blending and mixture ensure the unpacked ingredients are homogeneous so that finished product will be uniform composition. Lubricants are added before mixing to reduce friction and minimize die wear. Pressing usually conducted to form green compact. It consists of filling a die cavity with a controlled amount of blended powder, applying the required pressure and ejecting the as-pressed compact. Basically, this step is performed at room temperature. The pressure is varied to achieve the target density. The strength and density of compacted powder increase with pressure due to interlocking and plastic deformation. Along with increasing pressure, density reaches its plateau due to work-hardening and friction. Also, density decreases with increasing distance from pressing die surface. It is very difficult to reach full density. The last step, sintering, involves heating compacted powders in a controlled-atmosphere furnace to a temperature that is generally slightly below the melting point of the powder metal. It can produce strong bonding between powder particles, make chemical, dimensional or phase changes, and alloying if mixed elemental powders were used. Temperature, time and atmosphere are the most critical parameters in sintering. Temperature depends on what material is used. Proper sintering time ranges from 30 minutes to several hours. Commonly used atmosphere includes carbon monoxide, hydrogen and cracked ammonia.

There are many commonalities between powder metallurgy and friction stir consolidation process and few differences as well. Firstly, they both start from finely divided precursors and end up with a finished part. Unlike powder metallurgy, friction consolidation deals with not only metal powder but also metal wastes like machining chips. The surface finish of friction stir consolidated production may not as good as the part made by powder metallurgy. Secondly, great pressing force is required for achieving high density production. Thirdly, the high temperature is the key of bonding pieces together in both process. Fourthly, they both offer high material utilization efficiency because almost no scrap is lost. A major difference between them is friction consolidation is one-step process. Mixing, compacting and bonding almost performed together because the die is rotating with pressing force and the accompanying plastic deformation lead to heat dissipation and temperature rising. Blending tool, lubricants, furnaces and special sintering atmosphere are not required. This means friction consolidation process can save considerable time, labor, devices and space relative to conventional powder metallurgy. Also, the requirement of the quality of the precursor for friction stir consolidation is not a strict as powder metallurgy. Metal scrap like machining chips and dust are eligible for friction stir consolidation even if their sizes are highly uneven. So, a further saving of material can be made. However, it has to be mentioned that the production of powder metallurgy part is more precise and there is no need for further machining.

2.7 Effect of Chips Preparation on Friction Stir Processed parts

The quality of the recycled chip-based part produced by plastic deformation is highly altered by the methods when chips are prepared for consolidation at the early stage. Common factors to affect the chips preparation are, duration of pressing, pressure, recycling method, type of chips, and their morphology. Shazarel *et al.* (2016) founded that there was no a big quality difference between the extruded material from the hot and cold pressed chips. The raise in the pressing time or pressing pressure produces higher levels of consolidation. Low pressure Heat was used on granulated aluminum to reduce the spring back action and soften the particles. The result showed that the method was inferior by 2-13% in compressive strength, 18-29% in Brinell hardness and 9-12% in the green density as compared to the commercial aluminum powder method compressed at 360 MPa. Tekkaya *et al*. (2009) investigated the properties, drilling, yield behavior and microstructure of processed parts by FSP by direct hot extrusion of aluminum AA6060 alloy chips produced by turning and milling operations with different shapes and sizes. The mechanical properties of the seam welds surrounding the chips are nearly the same with property of the base material. The yield strength of the chips is comparable to the solid billet extrudate.

In general, the quality of the chip-based part is altered by the chips morphology if insufficient strain and stress are applied during the forming process. Therefore, minimum strain, stress, and temperature condition are needed to produce a metallic bonding regardless of different chip geometries.

2.8 Effect of Die Geometry in Friction Stir Processed Parts

The die geometry plays an enormous role to ensure a sound inter-particle chips bonding in the FSP. A proper die design will provide sufficient part densification, chip bonding and the evolution of desired microstructure (Shazarel *et al.* (2016)). The performance of the porthole and flat-face dies in direct recycling of AA6060 chips were also compared (Shazarel *et al.* (2016)). By porthole die, the chips welding and ductility is 80% greater than the flat-face die. Meanwhile the values of microhardness and the yield strength of the porthole die performed part are lower than its rival. The microstructure of the friction stir processed sample by the porthole die exhibited an equiaxed grains and counted almost twice than the grain size revealed by the flat-face die sample before the heat treatment. The effect of different routes of chip consolidation and dies design over mechanical properties are done by (Shazarel *et al.* (2016)). The AA6060 aluminum alloy chips were compacted into billets using three different methods namely traditional compaction in one stroke, multi-layer compaction and front-pad compaction adopted from powder extrusion. The multilayer compaction results in better density of a compacted chip. To sum up, the mechanical properties of the sample profile can be improved by proper design of die.

2.9 Optimisation of friction stir consolidation process using design of experiment

All products have certain characteristics which describe their performance relative to the requirements or expectations of their customers. The Taguchi method is one of the most widely applied robust design methods and enables a comprehensive understanding of the individual and combined effects of various design parameters to be obtained from a minimum number of experimental or simulation trials. By utilizing the Taguchi approach, product manufacturers and process designers can greatly improve the likelihood of the product (or process) satisfying the desired specification on a consistent basis. The basic principle of the Taguchi design method is to identify the parameter combination settings which affect the quality of the final product or process robust to unavoidable variations in external noise. The relative "quality" of a particular parameter design is evaluated using a generic signal-to-noise (S/N) ratio. Depending on the particular design problem, different S/N ratios are applicable, including "nominal is best" (NB), "lower is better" (LB), or "higher is better" (HB). In problems such as that considered in the current study, the objective is to identify the optimum input variable set up conditions which maximize the hardness and compression strength of the product, and hence the higher-is-better S/N ratio is applicable.

Li1 *et al.* (2017) studied the effect of applied load, rpm and consolidation time on the AA6061 and conducted DOE, they found a better consolidation at load 26700N, Speed 400 rpm and at consolidation time of 45 seconds.

2.10 Research Gaps

The literatures reviewed are describing about how the friction stir processing is preferable than conventional recycling method and how the effects of process parameters namely, temperature, deformation load are playing critical role in solid phase metal recycling.

Many research works have been conducted on friction stir processing by FSW and FSE. However, there are only few works are available on investigations of FSC process. Therefore the gaps observed in the literature are:

1. There was limitation on studying the effect of RPM, consolidation time and aspect ratios of compacted chip on the hardness and compression strength of the disk.
2. There were very limited literature on the study of thickness to diameter ratio for best consolidation, which can enhance the mechanical property of the disk.

In this research, the effect of diameter to thickness ratio (aspect ratio), rpm and consolidating time on the mechanical properties (hardness and compression strength) was investigated.

2.11 Summery of Literature Review

According to the reviewed literature, the power consumption required and hazards are minimum in friction stir processing or direct recycling than a conventional recycling techniques like casting. FSC is a single step process and more time, labor and material can be saved. Researches showed that high values of temperature, deformation and pressure play critical role in solid phase metal recycling. Post process analysis showed that high density and good mechanical properties can be achieved when sufficient extrusion pressure and temperature were utilized.

Chip size regardless of their geometry and the way chips are prepared has a significant effect on the qualities of the recycled part. Common factors influencing the chip preparation are pressure, duration of pressing, method of recycling, chip types and their morphology.

CHAPTER THREE: MATERIALS AND METHODS

3.1 Materials

The type of base material used in the present research was AA5052-TO (soft annealed) chips with an average thickness of 75 micrometer. The base material chemical composition is Aluminum alloy 5052 (Magnesium - 2.2%-2.8% by weight; Chromium - 0.15%-0.35% maximum; Copper - 0.1% maximum; Iron - 0.4% maximum; Manganese - 0.1% maximum; Silicon - 0.25% maximum; Zinc - 0.1% maximum). This alloy is medium strength soft annealed alloy that is commonly used in a wide variety of structures and marine applications (Oberg *et al.* (2008)).

3.1.2 Chips Preparation from AA5052

In order to prepare AA5052 chips with uniform size as precursors, desired thickness of AA5052 chip was made by milling machine model of FU281 based on Eq. (1) from 8mm diameter.

$$t_c = \frac{2v}{Nn}\sqrt{\frac{d}{D}} \qquad (3.1)$$

Where t_c is the average thickness of chips, N is the rotational speed of the cutter, n is the number of teeth on the cutter periphery, d is the depth of cut, D is the cutter diameter, and v is the linear speed (feed rate) of the workpiece (Li1 *et al.* (2017)). The parameters adopted to make chips with 76 μm average thickness are listed in Table 3.1. The actual thicknesses of the prepared chips were measured under a microscope. The average thickness is 75.8 μm with 8.3 μm as standard deviation. Accordingly, the chips were prepared as shown in (Figure 3.1) by using the parameters in Table 3.1 shown below.

Table 3.1 The parameters adopted for making 76 μm thick chips (Li1 *et al.* (2017))

N **(rev/s)**	***d*** **(mm)**	***v*** **(mm/s)**	***D*** **(mm)**	**Chip length (mm)**	***n***
2.13	0.5	2	19.05	3.18	4

Figure 3.1 Chips prepared for friction stir consolidation process

3.1.3 Density of a Pre-compacted Chips and Aspect Ratio Evaluation

A none rotating die with a stationary chamber and a flat backing plate at the bottom of the chamber was used to compress the chips to produce a precompacted disk. A pre-compacted chips had aspect ratio of 25.4/3 mm, 25.4/5 mm and 25.4/7 mm. Each of them had the same density of 2 g/cm^3 with different aspect ratios. Chips were pressed by the rotating die during stationary and added until the density reaches 2 g/cm^3 to the corresponding aspect ratio. The tool was not running during the compaction process.

The density of a compacted chips was obtained by using Archimedes principle. Weight in air and weigth in fluid of the compacted chips samples were obtained and given in Table 3.2.

Sample 1: 25.4/7 aspect ratio

W_{air} = 6.0305 gram

W_{fluid} = 3.01528 gram

Sample 2: 25.4/5 aspect ratio

W_{air} = 4.1625 gram

W_{fluid} = 2.08125 gram

Sample 3: 25.4/3 aspect ratio

W_{air} = 3.2682 gram

W_{fluid} = 1.7315 gram

Archimedes` principle states that the weight difference of the sample in air and in fluid is equals to the volume of the sample.

$$\text{Density} = \frac{W_{air}}{W_{air} - W_{fluid}} \tag{3.2}$$

In this research distilled water was used as a fluid whith density of 1g/cm^3.

$$\text{Density of sample 1} = \frac{6.0305g}{6.0305g - 3.01528g}$$

According to the Archemedes` principle, the weight difference in air and in water equals with the volume of the displaced water.

$$= 6.0305\text{g}/3.01522\ \text{cm}^3$$

$$= \underline{\underline{2.00002\ \text{g/cm}^3}}$$

$$\text{Density of sample 2} = 4.1625\text{g} / (4.1625\text{g} - 2.08125\text{g})$$

$$= \underline{\underline{2\ \text{g/cm}^3}}$$

$$\text{Density of sample 3} = 3.2682\text{g} / (3.2682\text{g} - 1.6341\text{g})$$

$$= \underline{\underline{2\ \text{g/cm}^3}}$$

Accordingly, the density of each samples are adjusted to 2 g/cm^3.

Table 3.2 Calculated densities of the three samples

Sample No.	**Aspect Ratio**	**Weight in air(g)**	**Weight in water(g)**	**Density(g/cm^3)**
1	25.4/7	6.0305	3.01525	2.00002
2	25.4/5	4.1625	2.08125	2
3	25.4/3	3.2682	1.6341	2

Figure 3.2 Weight in air of a compacted chip of aspect ratio 25.4/7

Then once after a density of 2g/cm^3 was obtained, the maximum pressing load and the weight of the chips required to achieve that density were recorded for each of the three aspect ratios (25.4/3, 25.4/5 and 25.4/7) to simplify the work for the next compaction process. (Figure 3.3) shows the three compacted chips at the density of 2 g/cm^3. These compacted chips were inserted in the chamber for FSC experiments carefully.

Figure 3. 3 Compacted chips

- To obtain the stated objectives in chapter one, the following methodology (shown in Figure 3.4) was implemented.

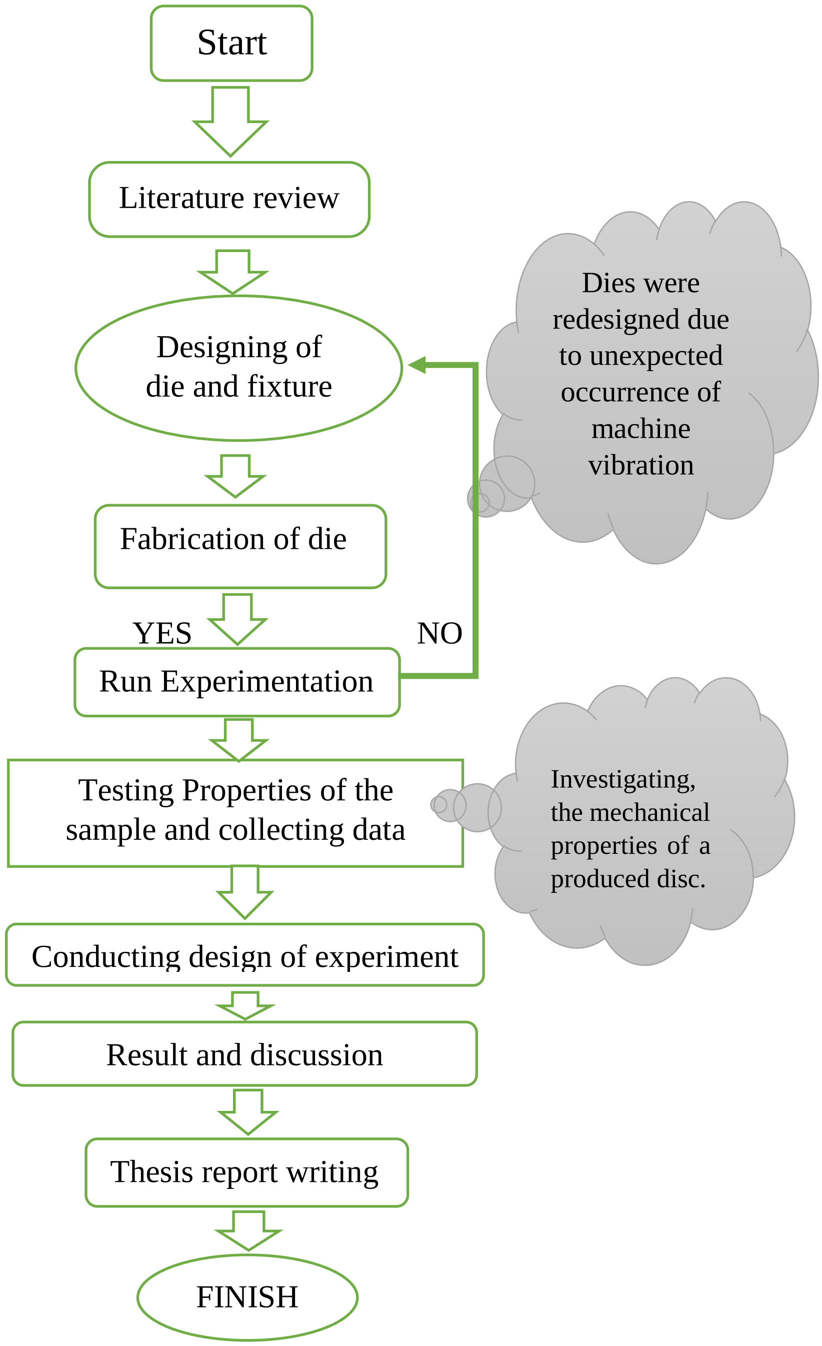

Figure 3. 4 Flow chart of the methodology of the research

3.2 Machines and Equipment

The equipment used in this study were rotating die, consolidation chamber, insert and chamber holder fixture. FSC set up having a rotating die, insert and chamber made of D2 tool steel and a chamber holding fixture made of steel 12050 grade was used for the trials experiment. The dimension of FSC dies used was diameter 25.38mm and height of 60mm, a consolidation chamber having internal diameter of 25.4mm and external diameter of 45.4, a chamber holder fixture dimension of 200mm x 300mm x 8mm and an insert of diameter 25.38mm and 30mm in height. The FSC trials were carried out by varying the rotating die speed (315 rpm, 400 rpm and 500 rpm), consolidating time (30, 45s and 60s) and compacted chip thickness (3 mm, 5 mm and 7mm) with a constant applied force of 2700N. In addition, a milling machine model of FU281 and pressure measuring device of DTZH was used as shown in Figure 3.7.

3.2.1 Geometrical Design and Manufacturing of Dies

The geometrical design of dies was carried out by SOLIDWORKS 2015 and the materials were selected based on data from literature. The materials used for the dies (i.e. rotating die, chamber and insert) were manufactured from D_2 tool steel and chamber holder fixture was manufactured from steel 12050. The circular shape of dies were made by using a conventional lathe machine and slots were constructed by using a conventional milling machine.

Experimental equipments namely consolidating chamber and rotating die were manufactured using conventional lathe and milling machine. The consolidating chamber was turned on a conventional lathe machine and slotted by using conventional milling machine. Rotating die was fabricated from a cylindrical part through turning and tapered on a conventional lathe machine by adjusting the tool post and finally slotted and drilled on a conventional milling machine. The insert was manufactured on a conventional lathe machine cut by saw machine and then faced on both sides and finally assembled on a milling machine FU281 as shown in Figure 3.5 and their exploded view is shown as in APPENDIX A. Once after the dies were assembled on the milling machine the next step was selecting the factors and levels combination and deciding the number of experiments required to run.

3.2.2 Experimental Procedure

The general experimental configurations and procedures of FSC are described as follows and also shown in Figure 3.5.

1) Align the chamber holder fixture and consolidation chamber with the rotational axis of the PDS or the rotating die and clamp the rotating die with PDS by using bolts. Further, align the pressure gauge`s piston with the insert.
2) Load the chamber with a pre-compacted chips.
3) Begin die rotation after the pressure was adjusted.

4) Once die rotation has begun and the spindle is rotating at the desired rate, the compaction force is raised to the desired level and maintained for the specified time.
5) Withdraw the die from the chamber and terminate the process.
6) Stop the rotation of the rotating die and press downward by the tool itself to remove the sample and the insert should be removed first.

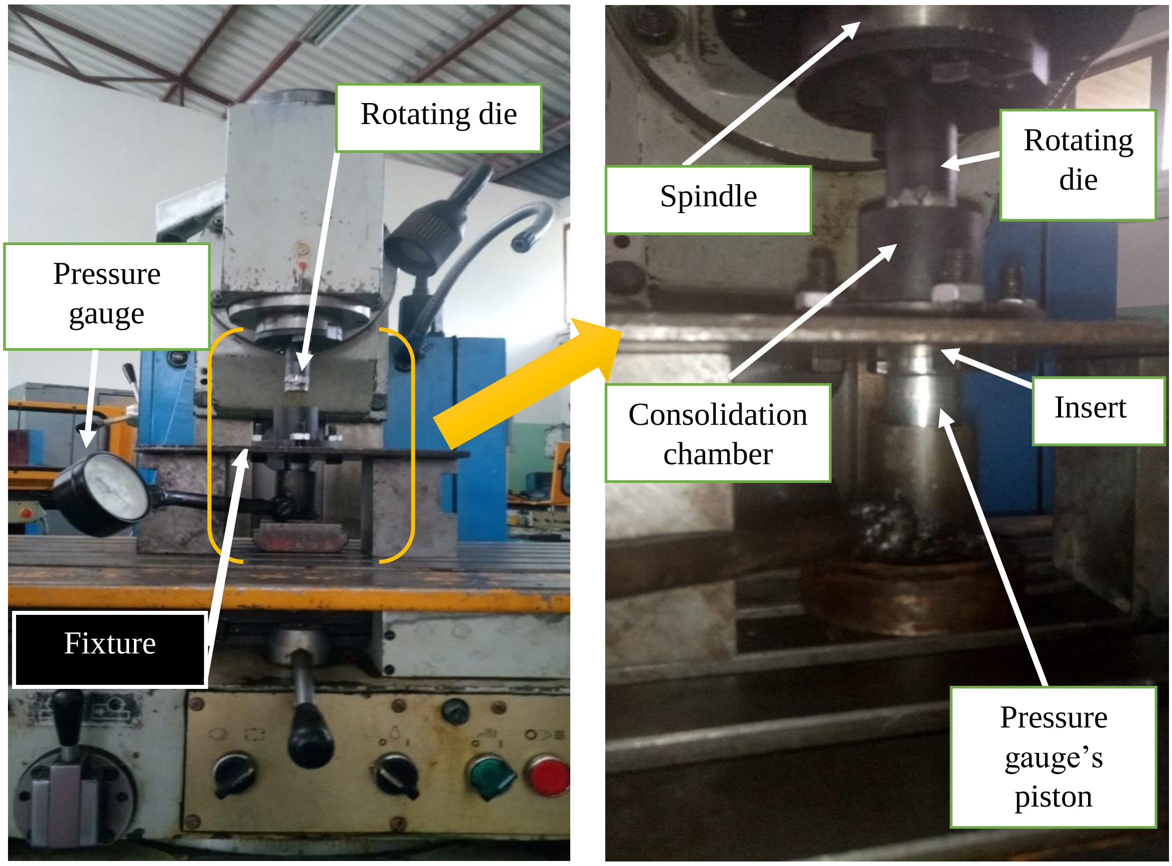

Figure 3. 5 Experimental set up of friction stir consolidation process

In these experiment, rotating die, chamber, insert and chamber holder fixture were used. The die materials that are rotating die, insert and consolidation chamber were fabricated from D2 tool steel and a backing plate was made from steel 12050. The rotating die was used in the experiment in which the die with 25.38 mm diameter and 60 mm in height and it was slotted at its top end in order to fix with the spindle of the milling machine. Chamber with the dimension of 25.4 mm in diameter and 50 mm in height were used with the insert of 25.38 diameter and height of 30 mm which is used as a support for the bottom side of a compacted chip and to allow the space for the pressure gauge. In addition, a chamber holder fixture with the dimension of 300 mm x 200 mm was used which is used as a fixture to support the chamber and keeps the chamber center for the rotating die. The chamber holder fixture was drilled at the midpoint to allow the physical contact between the pressure gauge and the insert which allows to measure the applied load as shown in (Figure 3.6) below.

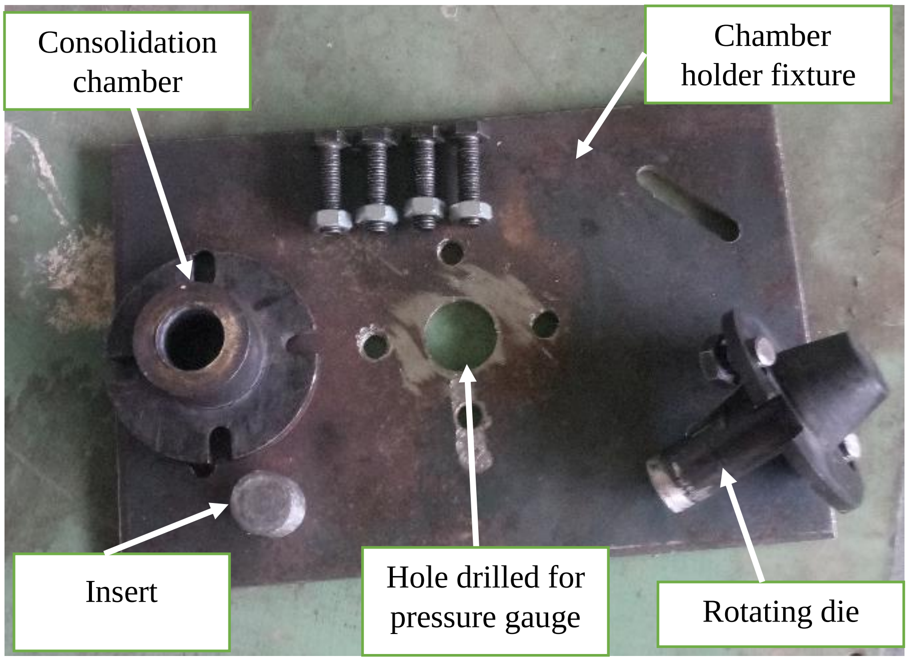

Figure 3. 6 Experimentation equipment.

3.2.3 Pressure Gauge Alignment and Gauge`s Reading

In order to quantify the applied load during the experimentation of FSC process, DTZH pressure gauge was used as shown in Figure 3.7. The pressure gauge`s piston was prepared to pass through the chamber holder fixture and directly contact with the insert. The fixture which holds the chamber from rotation was drilled to let the insert and pressure gauge`s piston contact each other.

The force was kept constant at 2700 N. The pressure read by the DTZH was converted into force based on (Shigley (2011)) :

$$P = \frac{F}{A} \tag{3.3}$$

where:

F is force applied by the insert which is 2700N

A is area of the pressure gauge`s piston which is equal to 900mm^2.

P is DTZH pressure gauge`s result which is 3 MPa.

Therefore, in order to maintain a force of 2700 N, the pressure gauge was kept raising the load until it reads 3 MPa then left in place until the desired time limit reaches.

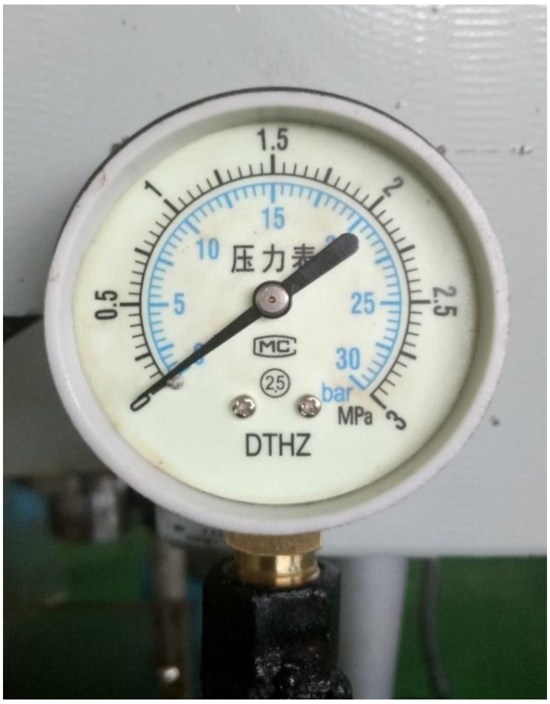

Figure 3. 7 The DTZH pressure gauge used for the experiment

3.3 Experimental Methods

3.3.1 Design of Experiment

The reason why design of experiment (DOE) is selected rather than the other approaches to conduct experiment is that it provides opportunity for systematic planning of experiments. Taguchi technique of DOE has been the most widely used technique for the last two decades. The benefit of DOEs is the ability to analyze the effect or “response” of many factors and levels with a minimum amount of experimentation. Factors are independent variables that are expected to affect the response variable whereas levels are the quantitative or qualitative settings which will be tested and one of the main disadvantage is that the optimum combination of process parameters and levels may not be available in the orthogonal array (OA) therefore, it requires additional experimentation for verification. One of the important steps involved in Taguchi’s technique is selection of orthogonal array. Which will further help to conduct experiments to determine the optimum level for each process parameters and establish the relative importance of individual process parameters. An OA is a small set from all possibilities which helps to determine least number of experiments. To obtain optimum process parameters setting, Taguchi proposed a statistical measure of performance called signal to noise ratio (Ross (1996)). This ratio considers both the mean and the variability of the process. In addition to S/N ratio, ANOVA is used to indicate the interaction influence of process parameters on performance measures. In addition, one of the most disadvantage of Taguchi`s method is that the optimum combination of the process parameters may not be available in the list of OA. Therefore, additional experiments for verification are required.

3.3.2 Full Factorial Design Method

A full factorial experiment is an experiment whose design consists of two or more factors, each with a discrete possible level and whose experimental units take all possible combinations of all those levels across all such factors. Such an experiment allows studying the effect of each factor on the response variable, as well as on the effect of interactions between factors on the response variable. A common experimental design is the one with all input factors set at two levels each. If there are k factors each at two levels; a full factorial design has 2^k runs. Thus for 6 factors at two level it would take 64 trials.

3.4 Taguchi Method

The full factorial design requires a large number of experiments to be carried out as stated above. It becomes laborious and complex, if the number of factors increase. To overcome this problem Taguchi suggested a specially designed method called the use of orthogonal array to study the entire parameter space with lesser number of experiment to be conducted. Taguchi thus, the use of loss function to measure the performance characteristics that are deviating from the desired target value. The value of this loss function is further transformed into signal-to-noise (S/N) ratio. Usually, there are three categories of the performance characteristics to analyze the S/N ratio. They are: nominal-the-best, larger-the-better, and smaller-the-better. And since the aim is increasing the response, larger the better is selected.

I. Steps Involved in Taguchi Method

The use of Taguchi`s parameter design involves the following steps

a. Identify the main function and its side effects.
b. Identify the noise factors, testing condition and quality characteristics.
c. Identify the objective function to be optimized.
d. Identify the control factors and their levels.
e. Select a suitable orthogonal array and construct the matrix.

f. Conduct the matrix experiment.

g. Examine the data; predict the optimum control factor levels and its performance.

h. Conduct the verification experiment.

II. Approach to the Experimental Design

In accordance with the steps that are involved in Taguchi`s method, a series of experiments are going to be conducted. Consolidation operation on AA5052 wastes using a milling machine has been carried out. The procedure is given below.

3.4.1 Identification of Main Function and its Side Effects

Main function: friction stir consolidation operation on AA5052 wastes using milling machine.

Side effects: variation in hardness and compression strength.

Before proceeding to the next steps, it is necessary to list down all the factors that affect or influence the friction stir consolidation process and from those factors it is important to identify the control and noise factors. The "factors" that affect friction stir consolidation process on a milling machine and associated uncontrollable factors (noise factors) are presented in the Table 3.3.

Table 3. 3 Factors that affect FSC operation

Control factors	Noise factors
Speed (rpm)	Machine condition and vibration
Aspect ratio(mm)	Operator skill
Time (s)	Temperature

After listing the control and the noise factors, decisions on the factors that significantly affect the performance are ascertained and only those factors was taken into consideration in constructing the matrix for experimentation. All other factors were considered as Noise Factors.

3.4.2 Identification of the Testing Conditions and Quality Characteristics to be observed

Quality Characteristics: mechanical property of the disk.

Workpiece Material: AA5052 alloy

Die Material: D_2

Operating Machine: Milling machine

Testing Equipment: Universal Testing Machine

3.4.3 Identification the Objective Function

Objective Function: Larger-The-Better

S/N Ratio for this function (Srinivas Athreya and Y.D.Venkatesh (2013)):

$$\text{S/N ratio } (\eta) = -10 \log_{10} \left(\frac{1}{n}\right) \sum_{i=1}^{n} \frac{1}{y_{ij}^2} \tag{3.4}$$

where, n is sample size, and y is Responses or yield (hardness and compression strength) in that run.

3.4.4 Identification of Control Factors and their Levels

The factors and their levels were decided for conducting the experiment based on information taken from a reviewed literature. Factors and levels are shown in Table 3.4.

Table 3. 4 Selected factors and their levels

FACTORS	**LEVELS**		
	1	**2**	**3**
Speed (rpm)	315	400	500
Aspect ratio (mm)	25.4/7	25.4/5	25.4/3
Time (s)	30	45	60

3.4.5 Selection of Orthogonal Array

To select an appropriate orthogonal array for conducting the experiments, the degrees of freedom are to be computed. The same is given below: MINITAB 17 was used for optimization.

Degrees of freedom: 1 for mean value, and 8= (2x4), two each for the remaining factors

Total degrees of freedom: 9

The most suitable orthogonal array for experimentation is L9 array as shown in Table 3.5.

Table 3. 5 Orthogonal Array (OA) L9

Experiment No.	Control Factors		
	1	**2**	**3**
1	1	1	1
2	1	2	2
3	1	3	3
4	2	1	3
5	2	2	1
6	2	3	2
7	3	1	2
8	3	2	3
9	3	3	1

3.4.6 Conducting the Matrix Experiment

In accordance with the above OA, experiments were conducted with their factors and their levels as shown in Table 3.5. The experimental layout with the selected values of the factors is shown in Table 3.6. Each of the 9 experiments was conducted 3 times (27 experiments in total) to account for the variations that may occur due to the noise factors. The compression strength and hardness values were determined using the universal testing machines.

Table 3. 6 OA with control factors for hardness

Experiment No.	Control Factors		
	Aspect ratio	**Speed (rpm)**	**Time(s)**
1	25.4/7	500	60
2	25.4/7	400	45
3	25.4/7	315	30
4	25.4/5	500	45
5	25.4/5	400	30
6	25.4/5	315	60
7	25.4/3	500	30
8	25.4/3	400	60
9	25.4/3	315	45

3.4.7 Disc sample Manufacturing

The disc samples were manufactured by optimum conditions or inputfactors. The specimens were fabricated by inserting a specified amount of chips (i.e. pre-compacted chips) into the consolidation chamber. Three trials were fabricated for each experimental conditions in the OA.

3.5 Sample Preparation and Testing Methods

3.5.1 Specimen Preparation for Hardness and microstructure Testing

The specimen preparation was conducted following the steps described below:

Step 1: Mounting (hot) ⇒ Grinding ⇒ Polishing

Step 2: Repolishing ⇒ Etching

Repolishing was conducted for further surface refinement and then etching was carried out to make the grain boundaries more visible. Figure 3.8 shows samples passing the steps namely mounting, grinding, polishing and repolishing steps and ready for etching. Etchants used for specimen preparation are shown in Table 3.7. Samples were immersed and soaked at average time of 34 seconds in the etchants and then soaked in the water for average time of 10 seconds. The samples were allowed to dry and taken to optical microscope.

Table 3. 7 Composition and conditions of etchants

Etchants	Composition	Condition
Methanol	25 ml	20 to 60 seconds
Hydrochloric Acid	25 ml	
Hydrofluoric Acid	One drop	
Nitric Acid	25 ml	

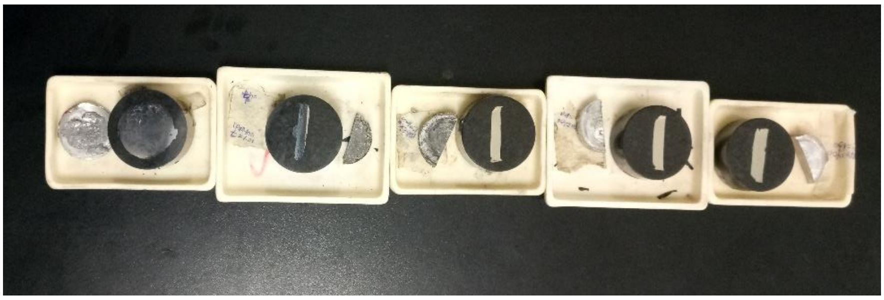

Figure 3. 8 Prepared samples passing mounting, grinding, polishing and re-polishing steps.

Step 3: Microstructural analysis

Step 4: Hardness testing

To reduce surface damage the specimen first sectioned by a cutting machine by abrasive cutter. Then cut part of the samples was mounted by using hot mounting press (model: RB 206 Metpress-A) and sand papers grades of 1200, 1400, 1600, 1800, and 2000 was used in the stated order to refine the surface. A model of (RB 204 Metpol-II) polishing machine was used to five rounds. Each round had 2 minutes to smoothen the surface and during this time, diamond abrasives of 6 micrometer metadi diamond suspension was used. Re-polishing was conducted for further surface refinement. Finally, etchants were used on the surface of the sample in order to make the surface microstructure easily seen by optical microscope of model (Huvitz HR-300 Series). The hardness was tested on the horizontal or radial cross section of the sample as shown in Figure 3.9 and each sample was tested at four different zones of the sample and the average was taken.

Figure 3. 9 Horizontal and vertical cross-section of the sample

The following Table 3.8 describes the process carried out from the beginning to the end of a sample preparation and machines used for testing of hardness and microstructure.

Table 3. 8 Sample preparation description

Steps	Process	Description	Machines used(models of machines)	Conditions
1	Sectioning	Type of cutters used: Abrasive cutter	RB 203 Abcut-M	Till sectioned
2	Mounting	Mounting type: hot compression mounting with resin.	RB 206 Metpress-A	Automatic
3	Grinding	Grit size of sand papers used: 1200, 1400, 1600, 1800 and 2000	Sand papers (manual)	Average of 8 strokes from 1200 to 2000
4	Polishing	Speed and suspension size used: 200Rpm, 6 µm diamond suspension	RB 204 Metpol-II	5 round, 2 minutes each
5	Repolishing	Speed and suspension size used: 200Rpm, 1 µm diamond suspension	RB 204 Metpol-II	4 round, 2 minute each
6	Etching	Etchants used: HCl, HNO_3, Methanol and HF	-	Soaked for average of 30 seconds

3.5.2 Calculations and Procedures of Vickers Hardness Test

In this research, Vickers hardness test was conducted due to its capability to test non-ferrous metals and their alloys. Kay *et al.* (2007) stated that Brinell hardness provides usable results up to HB=450, because higher test forces cause deformation of the indenter to begin to occur. Table 3.9 below shows the hardness ranges of non-ferrous metals and their alloys which lies in the range of 11-158. In addition, the conversion from Brinell hardness to Vickers hardness is: HB ~ 0.95 HV (Kay *et al.* (2007)). Therefore, Vickers hardness test is preferred accordingly.

Table 3. 9 Stress Level and Recorded Hardness Range for Various Materials (Kay G. *et al* (2007))

Stress level	**Hardness range, HB**	**Material**
30	70-600	Steel, iron > 140 HB
10	22-315	Ti, Ni, Co, Cu-alloys > 200 HB
5	11-158	Non-ferrous metals and their alloys
2.5	6-78	Bearing metals
1.25	3-39	Lead, tin

The Vickers hardness is calculated from the mean indentation diagonal length by using the following equation:

$$HV = 0.9272\frac{P}{A} = \frac{2P\,\sin(136°/2)}{d^2} \approx 1.8544\,\frac{P}{d^2} \qquad (3.5)$$

Where:

HV is Vickers hardness

P is Test force in kgf

d is arithmetical mean value of the measured indentation diagonals in mm For Vickers

A is Indentation surface in mm^2

Following the ASTM Standard Test Method for Vickers Hardness of Metallic Materials E 92, Vickers Hardness Tests are performed with test forces of from 1 to 120 kgf. (Kay G. et al (2007)). Accordingly, testing was conducted using load of 10 kgf and held for 10 seconds in the principles given in Figure 3.10.

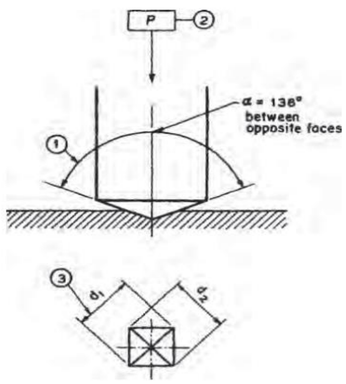

Figure 3. 10 Vickers hardness testing, test principle ASTM Standard E 92 (Kay *et al.* (2007)).

3.5.3 Grain Size and Microstructural Investigation

The microstructure of the sample was observed by using optical microscopy (HR-300 Series). Methods used to quantify the average grain size of the disk was line intercept method. Average grain sizes were determined by using ASTM E112-13 standard shown as in See APPENDIX B.

3.5.4 Compression Strength Testing of the Sample

Compression strength was tested by using universal testing machine as shown in Figure 3.11 below.

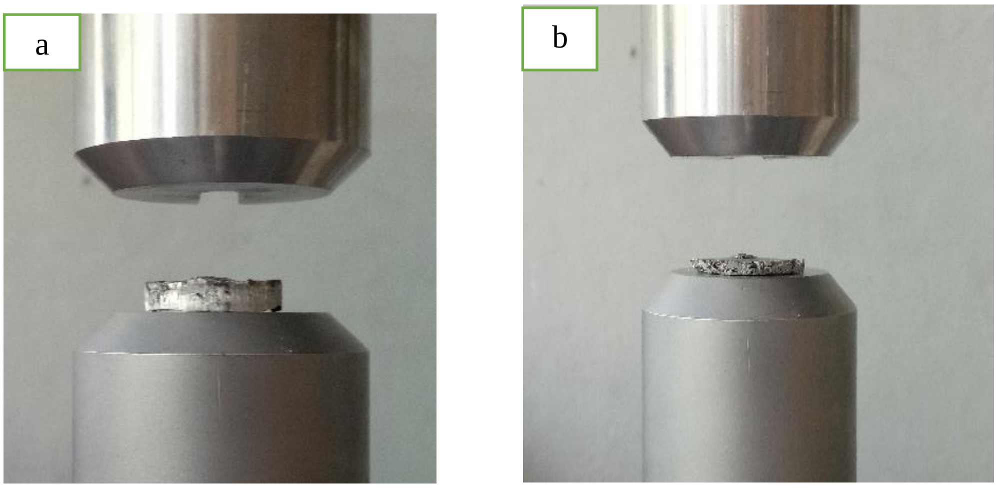

Figure 3. 11 Compression testing a) before test b) after test

3.6 Data Analysis

In this research, quantitative data was collected from experimentally tested values. Based on the experimentally collected data, the data analysis and interpretation were made by using MINITAB 17 software.

CHAPTER FOUR: RESULTS AND DISCUSSIONS

4.1 Experimental Results

The fabrication of discs through friction stir consolidation process was successfully performed on a milling machine model FU 281. Figure 4.1 shows the results of the three different aspect ratios fabricated on a milling machine by varying the process parameters. There are minimum flashes produced on the discs edge due to the presence of clearance between the chamber and rotating die. This flashes were filed before the specimens were tested. Aspect ratios previously had 3mm, 5mm and 7mm thickness at their green compacted level with diameter of 25.4mm.

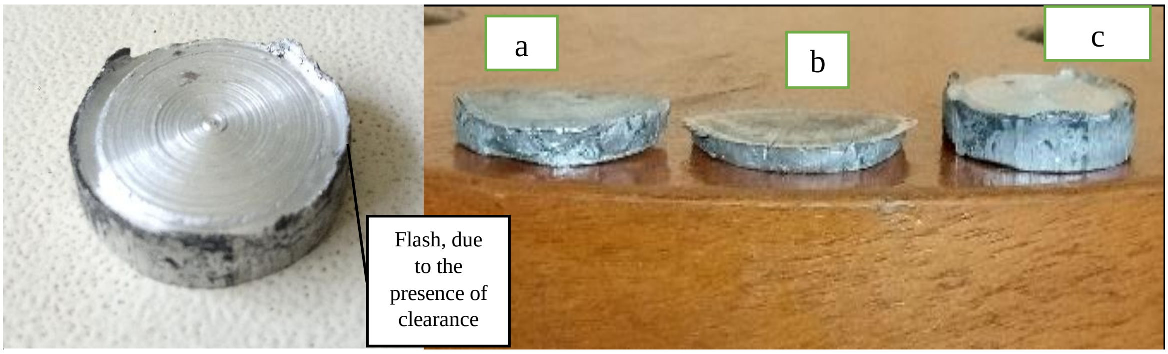

Figure 4. 1 Result of produced discs at different aspect ratio a) 25.4/5 b) 25.4/3 c) 25.4/7

4.2 Hardness Test Results

Test results of the three experiments hardness with their calculated values of signal to noise ratio and mean are listed in Table 4.1 below.

Table 4. 1 Hardness test results with their calculated S/N and MEAN results

No.	Aspect Ratio	Speed	Time	E 1	E 2	E 3	SD	S/N Ratio	MEAN
1	25.4/7	500	60	45.5	44.2	43.1	1.20139	32.9152	44.2667
2	25.4/7	400	45	43.3	42.5	40.6	1.38684	32.4829	42.1333
3	25.4/7	315	30	40.1	41.0	42.5	1.21244	32.2905	41.2000
4	25.4/5	500	45	46.6	45.8	47.7	0.95394	33.3827	46.7000
5	25.4/5	400	30	45.2	44.9	45.0	0.15275	33.0706	45.0333
6	25.4/5	315	60	46.6	46.0	45.5	0.55076	33.2602	46.0333
7	25.4/3	500	30	50.2	48.6	48.9	0.85049	33.8426	49.2333
8	25.4/3	400	60	52.1	50.1	52.1	1.15470	34.2204	51.4333
9	25.4/3	315	45	50.0	47.8	49.8	1.21655	33.8339	49.2000

As it is observed from the Table 4.1 that, mean HV values of the three trials are higher at combinations of experiment number eight (i.e. 25.4/3, 400 and 60) and average of 51.433 HV was recorded. Minimum values of HV is observed at the experiment number three, about an average of 41.2000 HV. It can be seen from the Table 4.1 that at aspect ratio of 25.4/7, the average HV values are lower than the other aspect ratios (i.e. 25.4/5 and 25.4/3) that is below 44.2667 HV. The higher Vickers hardness values are obtained at aspect ratios of 25.4/3 (i.e. above 49.2000 HV). This shows that, regardless of time and speed, the variation in aspect ratio results in variation hardness values.

4.3 Main Effect Plots

4.3.1 Main Effect Plot for S/N Ratio

According to the present work, the result of MINITAB 17 shows that, the experimental result demonstrates that aspect ratio and time are the significant factors or parameters that influence the hardness of the consolidated sample as shown in Table 4.3.

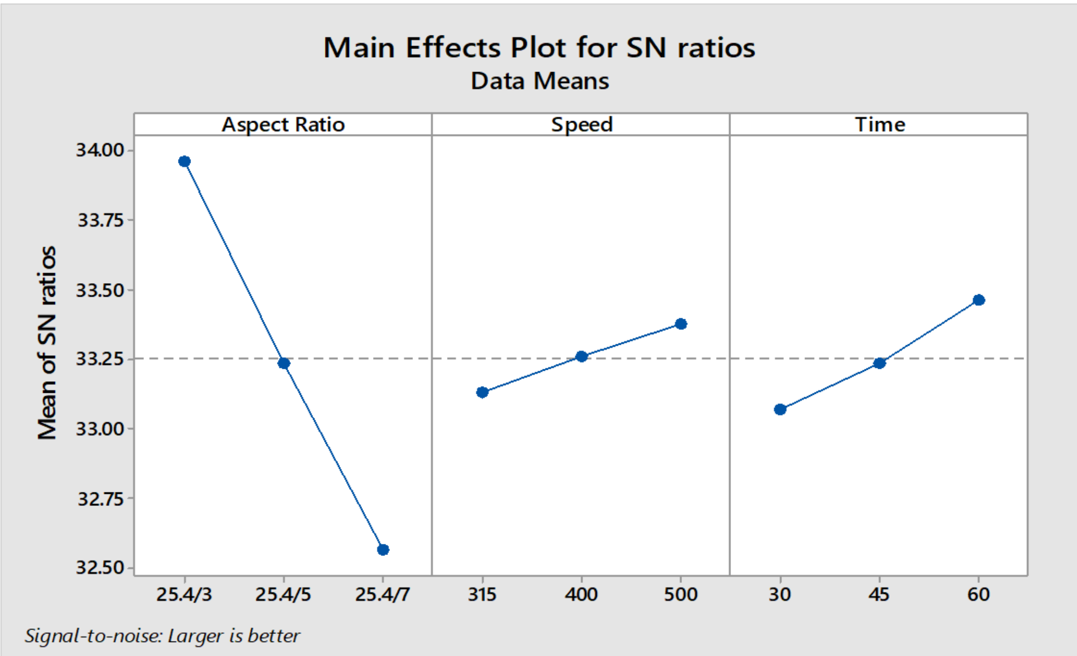

Figure 4. 2 Main effect plot for S/N ratio for hardness

The larger is better main effect plot for S/N ratio shown in Figure 4.2 shows that the values of S/N ratio are higher at aspect ratio, speed and time at 25.4/3, 500rpm and 60s respectively. The S/N ratio of hardness response is minimum at the combinations of aspect ratio at 25.4/7, speed at 315rpm and time at 30s. The objective is maximizing the response. Therefore, based on main effect plot for S/N ratio the optimum combinations are selected as aspect ratio, speed and time at 25.4/3, 500rpm and 60s respectively. The result of main effect plot for signal to noise ratio of MINITAB 2017 reveals that the optimum set up of input parameters are listed in Table 4.2 However these input parameters set up do not exist in an orthogonal array and not experimented. Therefore, confirmation experiment is required. Accordingly, it was experimented and tested as shown in Table 4.5.

Table 4. 2 Optimum combination of input parameters for verification of FSC process on hardness response

Aspect ratio	Speed (rpm)	Time (s)
25.4/3	500	60

From the Table 4.3 it can be seen that the influence rank of each factor on the hardness response can be interpreted as the effect of aspect ratio on the hardness takes the first rank, whereas time and speed takes the second and third rank respectively.

Table 4. 3 Response table for Signal to Noise Ratio Larger is better

Level	Aspect Ratio	Speed	Time
1	33.97	33.13	33.07
2	33.24	33.26	33.23
3	32.56	33.38	33.47
Delta	1.40	0.25	0.40
Rank	1	3	2

From Table 4.3 it can be seen that the rank of each factors effect are given. However, to what contribution does each factors influence on the hardness or response is shown in Figure 4.3.

```
Analysis of Variance for Transformed Response

Source           DF   Seq SS  Contribution
  Speed           2  0.11835         5.32%
  Aspect Ratio    2  1.72872        77.69%
  Time            2  0.09504         4.27%
Error             2  0.28298        12.72%
Total             8  2.22509       100.00%
```

Figure 4. 3 Percentage contribution of control factors on hardness

From result of MINITAB 17 depicted in Figure 4.3, it can be seen that speed, aspect ratio and time having percentage contribution of 3.63%, 88.33% and 7.61% respectively with error percent of 0.43%.

4.3.2 Main Effect Plot for Means

Main effect plot for means of Figure 4.4 describes the mean Vickers hardness values based on the raw data obtained from the experimentation. Based on the raw data main effect plot for means also confirms the result of signal to noise ratios. It also predict the same result as S/N ratio for optimum process parameter combinations. The optimum process parameter combinations can be listed out based on the Figure 4.4 as aspect ratio at 25.4/3, speed at 500rpm and time at 60s are the optimum combination of process parameters.

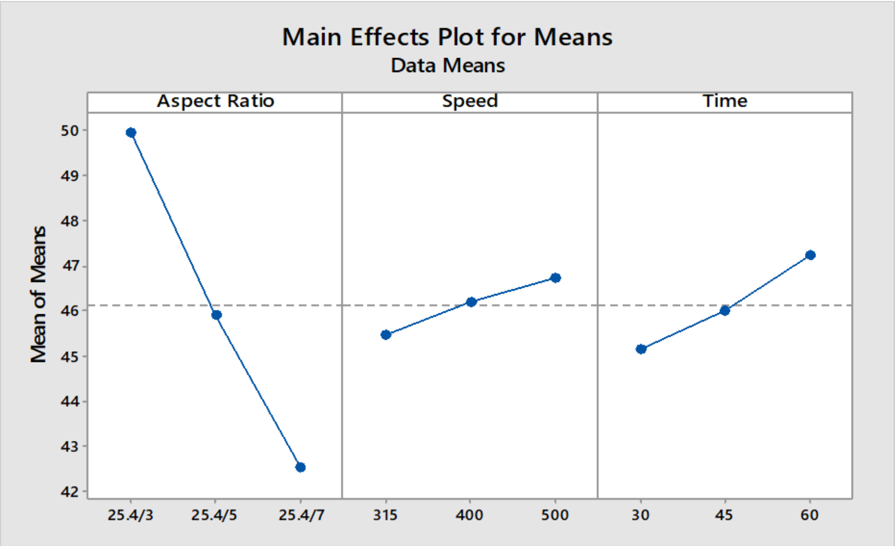

Figure 4. 4 Main effect plot for means

The effect of each factors on the hardness response is predicted by MINITAB 17 as shown in Table 4.4. Aspect ratio has significant effect on the hardness as compared to time and speed.

Table 4. 4 Response table for means

Level	Aspect Ratio	Speed	Time
1	49.96	45.48	45.16
2	45.92	46.20	46.01
3	42.53	46.73	47.24
Delta	7.42	1.26	2.09
Rank	1	3	2

The ranks exposed by MINITAB 17 based on the raw data or mean in Table 4.4, that aspect ratio has significant effect on the hardness as compared to speed and time.

4.4 Interaction plot Analysis for Signal to Noise Ratio

According to MINITAB 2017 result of interaction plot for signal to noise ratios, the effect of time, aspect ratio and speed on the yield (hardness) is analyzed as:

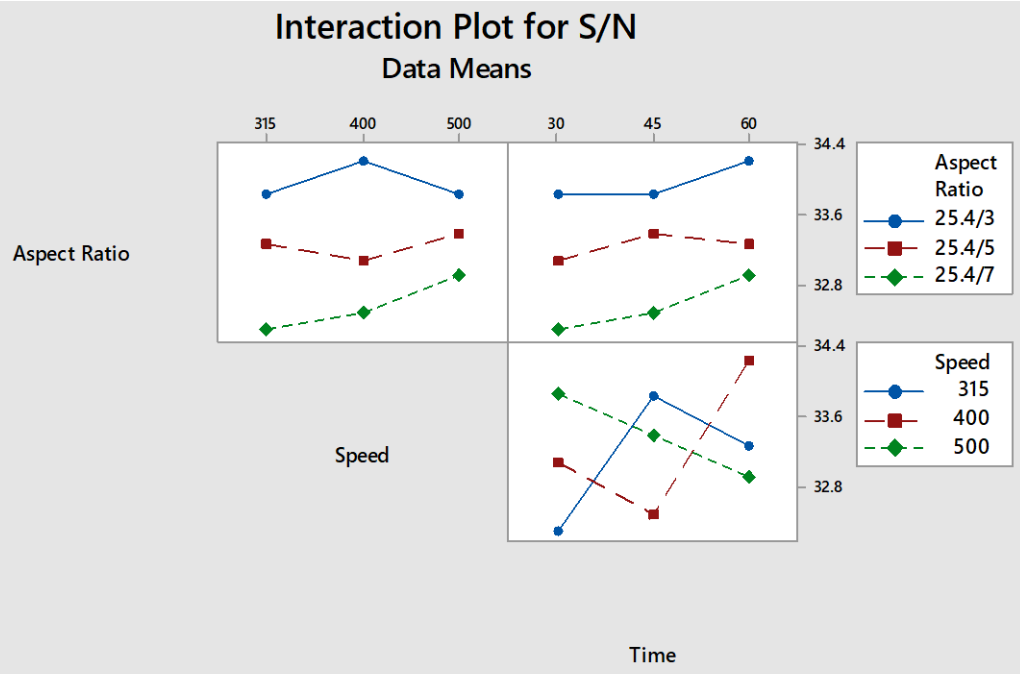

Figure 4. 5 Interaction plot analysis for S/N on the hardness

Based on the Figure 4.5 the following discussions can be pointed out for the interaction of aspect ratio versus time, speed versus time and speed versus aspect ratios as follows.

4.4.1 Interaction Plot Analysis of Aspect Ratio and Time on the Hardness

- Hardness is minimum at time of 30 seconds with aspect ratios of 25.4/7 and hardness is maximum at time of 60 seconds with aspect ratios of 25.4/3.
- At aspect ratio of 25.4/7 the hardness is maximum, medium and minimum at time of 60 seconds, 45 seconds and 30 seconds respectively.
- When the aspect ratio is at 25.4/5 the hardness is maximum, medium and minimum at at time of 45 seconds, 60 seconds and 30 seconds respectively.
- When the aspect ratio is 25.4/3 the hardness gets maximum, medium and minimum values at time of 60 seconds, 45 seconds and 30 seconds respectively.

4.4.2 Interaction Plot Analysis of Speed and Time on the Hardness

- At speed of 315 rpm the hardness is maximum, medium and minimum at time of 45 seconds, 60 seconds and 30 seconds respectively.
- When the speed is 400 rpm the hardness is maximum, medium and minimum at time of 60 seconds, 30 seconds and 45 seconds respectively.
- At speed of 500 rpm the hardness is maximum, medium and minimum at time of 30 seconds, 45 seconds and 60 seconds respectively.

4.4.3 Interaction Plot Analysis of Speed and Aspect Ratio on the Hardness

- At speed of 315 rpm the hardness is maximum, medium and minimum at aspect ratios of 25.4/3, 25.4/5 and 25.4/7 respectively.
- At speed of 400 rpm the hardness is maximum, medium and minimum at aspect ratios of 25.4/3, 25.4/5 and 25.4/7 respectively.
- When the speed is 500 rpm the hardness is maximum, medium and minimum at aspect ratios of 25.4/3, 25.4/5 and 25.4/7 respectively.

4.5 Contour Plot of Speed versus Time

According to contour plot the mean hardness values of Vickers hardness of the samples increases as the consolidation time or speed increases. In addition to this, it is important to mention about the influence of time versus speed on the mean values of Vickers hardness because of they have related or comparable values of percentage contribution on the hardness.

It can be pointed out from the Figure 4.6 that the Vickers hardness is maximum or above 50 HV at speed of ranging from 360 rpm to 450 rpm with corresponding time of ranging from 57 to 60 seconds. Likewise, HV is minimum or below 42, at speed of ranging from 380 to 440 with the corresponding time of ranging from 36 to 44 seconds. Therefore, it can be right to conclude as they have interrelated relationship to each other.

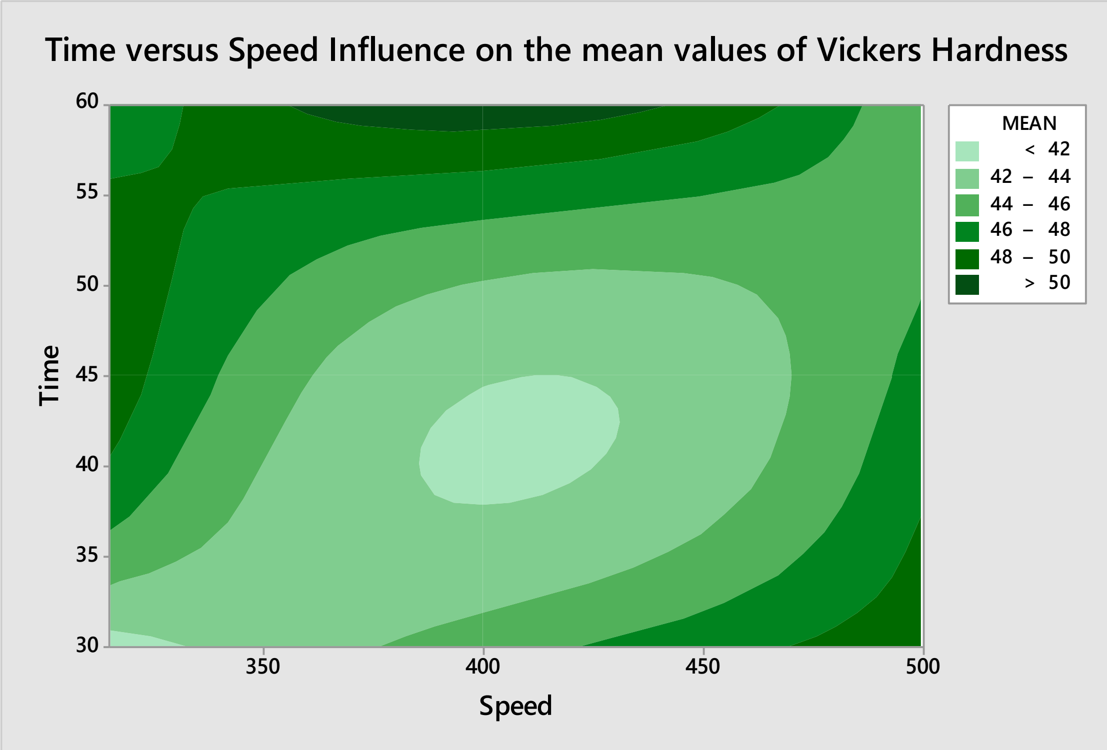

Figure 4. 6 Influence of time versus speed on the mean values of HV.

Because it is possible to produce a disc having 48-50 HV values by taking minimum time with higher speed (30s and 500rpm) and by taking maximum time with lower speed (60s and 315rpm).

4. 6 Confirmation Experiment

The experimental confirmation test is the final step in verifying the results drawn based on Taguchi's design approach. The optimal conditions are set for the significant factors and a selected number of experiments are run under specified FSC conditions. The average of the results from the confirmation experiment is compared with the predicted average based on the parameters and levels tested. The confirmation experiment is a crucial step and is highly recommended by Taguchi to verify the experimental results (Ross PJ (1996)). The final step of the DOE is the confirmation test, which verifies if the optimum conditions suggested by the matrix experiment do indeed give the improvement projected. The verification experiment is performed by conducting a test with optimal settings of the factors and levels previously evaluated. The confirmation experiments were conducted by adjusting the optimum set ups revealed by MINITAB 17 of Signal to noise ratios (i.e. 25.4/3 500Rpm 60s) in three trials to verify optimal friction stir consolidation process for hardness response.

Table 4. 5 Verification experiment result on hardness response

Exp. No.	Aspect ratio	Speed (rpm)	Time (s)	E 1	E 2	E 3
1	25.4/3	500	60	52.9	52.4	54.3

Experimental test result in Table 4.5 shows that friction stir consolidation process for AA5052, use of high speed, high aspect ratio and extended time are recommended to obtain better hardness for the specific range at speed of 500 rpm, aspect ratio of 25.4/7 and time of 60 seconds. In addition, the signal to noise ratio and mean are calculated manually according to eq. (3.4) for S/N larger is better. The result shows that mean and signal to noise ratio were obtained as 53.2 and 34.5152 respectively.

$$\text{S/N ratio } (\eta) = -10 \log_{10} \left(\frac{1}{n}\right) \sum_{i=1}^{n} \frac{1}{y_{ij}^2} \quad (3.4)$$

$$\text{S/N} = -10 \log_{10} \left(\frac{1}{3}\right) [\left(\frac{1}{52.9}\right)^2 + \left(\frac{1}{52.4}\right)^2 + \left(\frac{1}{54.3}\right)^2]$$

$$\text{S/N} = -10 \log_{10} [0.0003535666]$$

$$\text{S/N} = \underline{34.5152}$$

$$\text{Mean} = \left(\frac{52.9+52.4+54.3}{3}\right) = \underline{\underline{53.2}}$$

The signal to noise ratio and mean result shows that the optimum parameter obtained by Taguchi is reliable and consistent. Total three sets of experiment were conducted and their hardness values were checked. It can be seen that the results are consistent.

4.7 Compression Test Result

Compression strength test results of the nine numbers of experiments with their respective trials (i.e. T1, T2 and T3) and their calculated values of mean and aspect ratio is listed in Table 4.6 as shown below. Based on the raw data of compression strength test results as listed in Table 4.6, it can be seen that the mean values of compression strength is higher at process parameter combination of experiment number seven (i.e. speed at 500rpm, aspect ratio at 25.4/3 and time at 60s) resulting about 130.437 MPa. Compression strength is lower at combinations of experiment number nine (i.e. at speed, aspect ratio and time of 500rpm, 25.4/7 and 45s respectively).

Table 4. 6 Experimental test results for Compression Strength

No.	Speed	Aspect Ratio	Time	E 1	E 2	E 3	SD	S/N	MEAN
1	315	25.4/3	30	130.09	115.63	124.45	7.28805	41.7947	123.390
2	315	25.4/5	45	118.62	120.23	116.21	2.02322	41.4611	118.353
3	315	25.4/7	60	112.53	119.65	114.05	3.74977	41.2359	115.410
4	400	25.4/3	45	126.63	126.88	129.66	1.68185	42.1239	127.723
5	400	25.4/5	60	118.55	122.68	120.04	2.09151	41.6116	120.423
6	400	25.4/7	30	112.61	116.67	108.12	4.27680	41.0079	112.467
7	500	25.4/3	60	134.65	128.44	128.22	3.65051	42.3013	130.437
8	500	25.4/5	30	130.14	129.55	127.00	1.66884	42.2034	128.897
9	500	25.4/7	45	109.61	111.22	110.44	0.80513	40.8608	110.423

The variation in aspect ratio affects the compression strength of the disk significantly. The variation of speed and time do not have significant effect on the compression strength.

4.8 Main Effect Plot

Mainly, the main effects is taken from plot of signal to noise ratio and confirmed by plot of mean because main effect plot for means predicts the compression strength based on the raw data without considering maximizing the results.

4.8.1 Main Effect Plot for Signal to Noise Ratio of Compression Strength

Main effect plot for signal to noise ratio, as shown in Figure 4.7.

- As the aspect ratio increases the compression strength of the consolidated sample increases. Because the heat can easily transfers from the top surface of the disc to the remote areas of the disc and strong inter-chip welding is maintained at the bottom surface of the disc.
- When the speed increases the compression strength of the consolidated sample increases.
- The compression strength of the consolidated sample increases at time of 60 seconds and 30 seconds but minimum at time 45 seconds. Because at higher consolidation time, sufficient heat will be produced. This heat results in weldments of chips at the

remote areas of the disc. The stronger the weldment of chip results in increased compressive strength

According to the main effect plot for signal to noise ratio, the optimum set up of three levels and the three factors are given below in Table 4.7. Therefore, these optimum set up is experimented in an orthogonal array of Table 4.6 row 7th or experiment number seven.

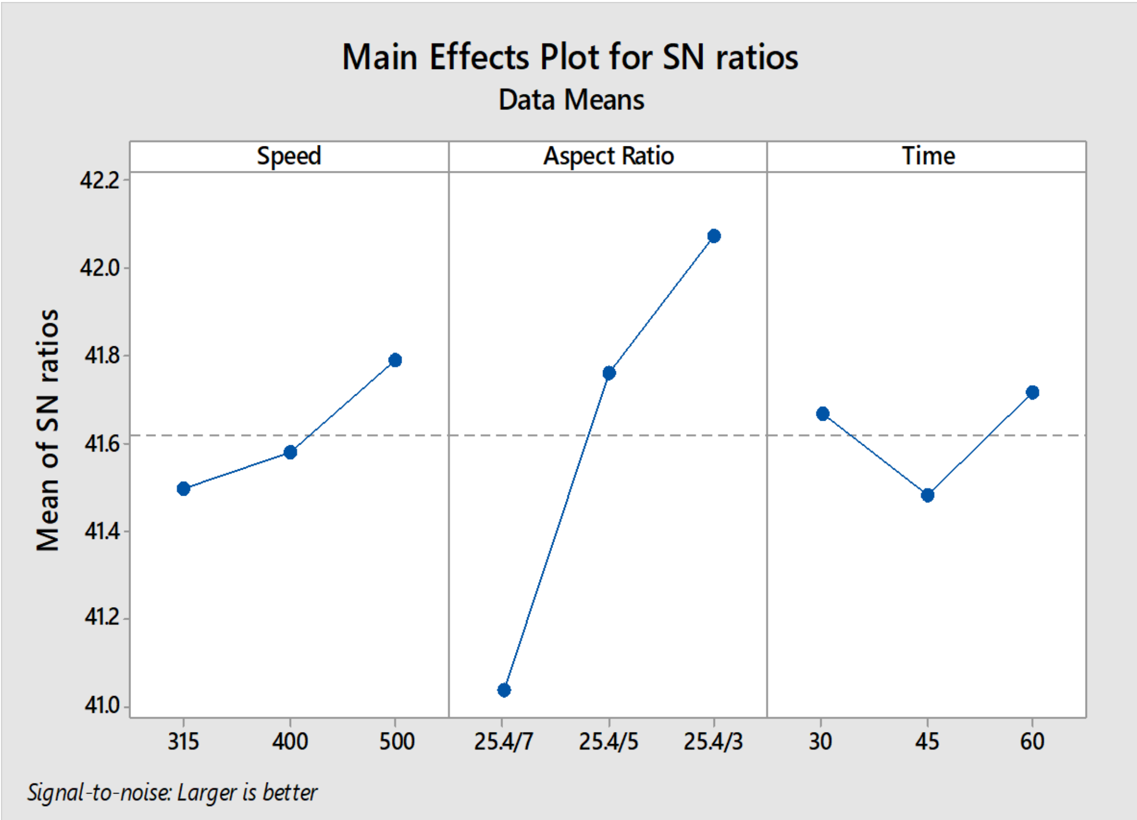

Figure 4. 7 Main effect plot for S/N ratio

The optimum parameter combination predicted by main effect plot for S/N ratios is shown in Table 4.7 as the speed, aspect ratio and time at 500rpm, 25.4/3 and 60s respectively. Therefore to get a better compression strength, the combination are set to be at 500rpm, 25.4/3 and 60s as predicted by MINITAB 17 software.

Table 4. 7 The optimum setup of factors and levels for compression strength

Factors	**Speed(rpm)**	**Aspect ratio**	**Time (s)**
Levels	500	25.4/3	60

Response table for Signal to noise ratio for Larger is the better shows that for a compression strength of a consolidated sample, aspect ratio and speed have the highest influence while time has a less influence. According to MINITAB 17, result provided in Table 4.8 depicts the influence of each level on the compression strength which is given as aspect ratio first rank, speed second rank and time as the third rank.

Table 4. 8 Response Table for Signal to Noise Ratios for larger is better

Level	Speed	Aspect ratio	Time
1	41.50	42.07	41.62
2	41.58	41.76	41.48
3	41.79	41.03	41.72
Delta	0.29	1.04	0.23
Rank	2	1	3

4.8.2 Main Effect Plot for Means

The main effect plot of mean also shows that the optimum set up of friction stir consolidation is at: speed of 500 rpm, aspect ratio of 25.4/7 and time of 60 seconds. Based on the mean results, Figure 4.8 analyzed as:

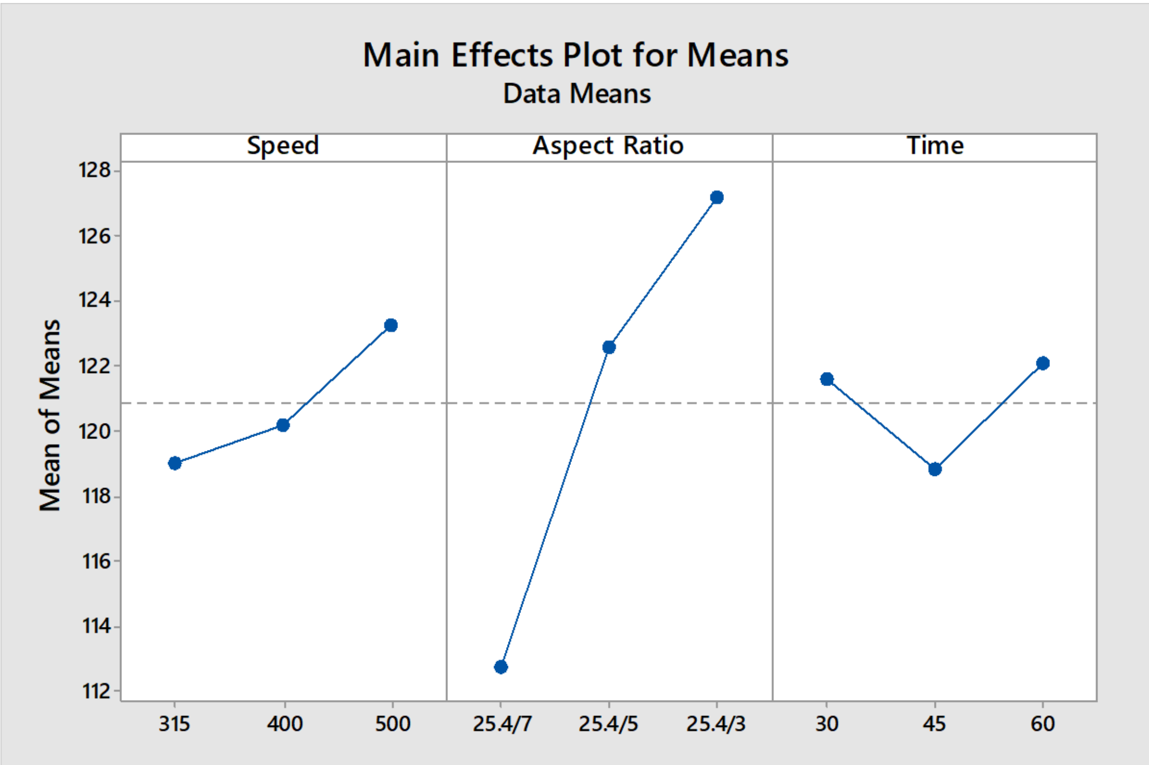

Figure 4. 8 Main effect plot for Mean results of compression strength

- The compression strength of the specimen is greater when the speed is at 500 rpm, lower when the speed is at 315 rpm and medium when the speed is at 400 rpm.
- Again the compression strength is greater at aspect ratio of 25.4/7, medium at 25.4/5 and lower at 25.4/3. This shows that as the thickness of the disc sample increases the compression strength decreases.
- The compression strength is greater at time of 60 seconds and lower at time of 45 seconds.

Table 4. 9 Response table for mean

Level	**Speed**	**Aspect ratio**	**Time**
1	119.1	112.8	121.6
2	120.2	122.6	118.8
3	123.3	127.2	122.1
Delta	4.2	14.4	3.3
Rank	2	1	3

Depending on mean results listed in Table 4.9, it can be seen that the effect of aspect ratio is higher as compared to speed and time. Response table for means confirmed the results predicted by signal to noise ratio.

```
Analysis of Variance for Transformed Response

Source          DF   Seq SS  Contribution
  Speed          2  0.11835         5.32%
  Aspect Ratio   2  1.72872        77.69%
  Time           2  0.09504         4.27%
Error            2  0.28298        12.72%
Total            8  2.22509       100.00%
```

Figure 4. 9 Percentage contribution of control factors on the compression strength

Figure 4.9 depicts speed, aspect ratio and time having percentage contribution of 5.32%, 77.69% and 4.27% respectively with error percent of 12.72%.

4.9 Interaction plot Analysis for Signal to Noise Ratio

According to interaction plot analysis for signal to noise ratio the interaction effect of aspect ratio and time, speed and aspect ratio, time and speed on the compression strength is analyzed.

4.9.1 Interaction Plot Analysis of Aspect Ratio and Time

It can be concluded from the Figure 4.10 as:

- The compression strength of the sample is maximum, medium and minimum at aspect ratio of 25.4/7 and time of 60 seconds, 30 seconds and 45 seconds, respectively.
- At aspect ratio of 25.4/5 the compression strength is maximum, medium and minimum at time of 30 seconds, 60 seconds and 45 seconds, respectively.
- When the aspect ratio is 25.4/3 the compression strength is maximum, medium and minimum at time of 60 seconds, 45 seconds and 30 seconds, respectively.

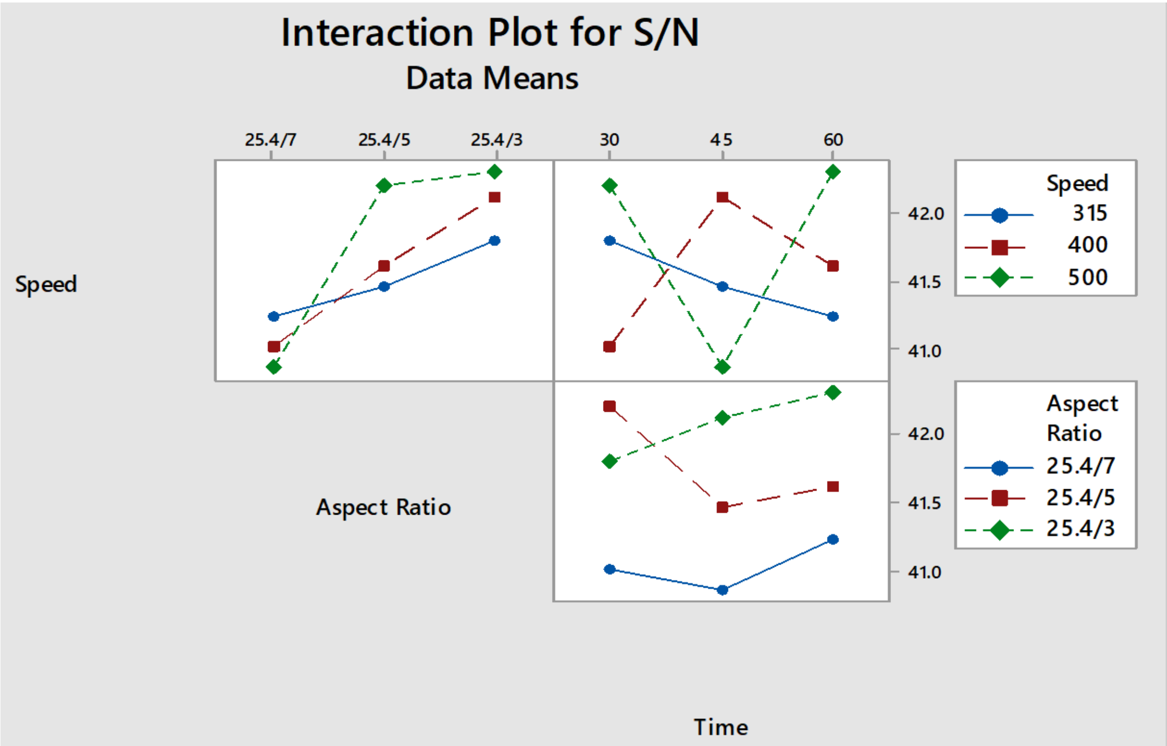

Figure 4. 10 Interaction plot for signal to noise ratio

4.9.2 Interaction Plot Analysis of Speed and Aspect Ratio

From the Figure 4.10 the interaction of speed and aspect ratio is analyzed as:

- At speed of 315 rpm the compression strength is maximum, medium and minimum at aspect ratios of 25.4/3, 25.4/5 and 25.4/7 respectively.
- When the speed is 400 rpm the compression strength is maximum, medium and minimum at aspect ratios of 25.4/3, 25.4/5 and 25.4/7 respectively.
- At speed of 500 rpm the compression strength is maximum, medium and minimum at aspect ratios of 25.4/3, 25.4/5 and 25.3/7 respectively.

4.9.3 Interaction Plot Analysis of Time and Speed

Relying on Figure 4.10 the interaction effect of time and speed can be described as:

- At time of 30 seconds, the compression strength is maximum, medium and minimum at speeds of 500 rpm, 315 rpm and 400 rpm respectively.
- When the time is 45 seconds, the compression strength is maximum, medium and minimum at speeds of 400 rpm, 315 rpm and 500 rpm respectively.
- At time of 60 seconds the compression strength is maximum, medium and minimum at speeds of 500 rpm, 400 rpm and 315 rpm respectively.

4.10 Contour Plot of Speed versus Time

It can be seen from the Figure 4.11 that the influence of time versus speed on the compression strength is highly interrelated and comparable. MINITAB 17 contour plot revealed that, the higher the speed does not have a significant influence on the improved compression strength as long as it is possible to fabricate a disc having improved compression strength with speed of 400 rpm and time 55 seconds. It can be pointed out from the Figure 4.11 that at 400 rpm there are compression strength less than 115 MPa and from 125-130 MPa at time of 30 seconds and 40 to 55 seconds. This shows that speed requires the help of time to achieve higher compression strength.

As the speed increases the compression strength of the sample increases at speeds of starting from 350 rpm to 450 rpm, then after some point it decreases even if time increases. Finally the compression strength increases starting from 460 rpm to 500 rpm with respective time ranging from 57 to 60 seconds. It is also observed from the plot that at 500 rpm and 30 seconds the compression strength gets 125 – 130 MPa.

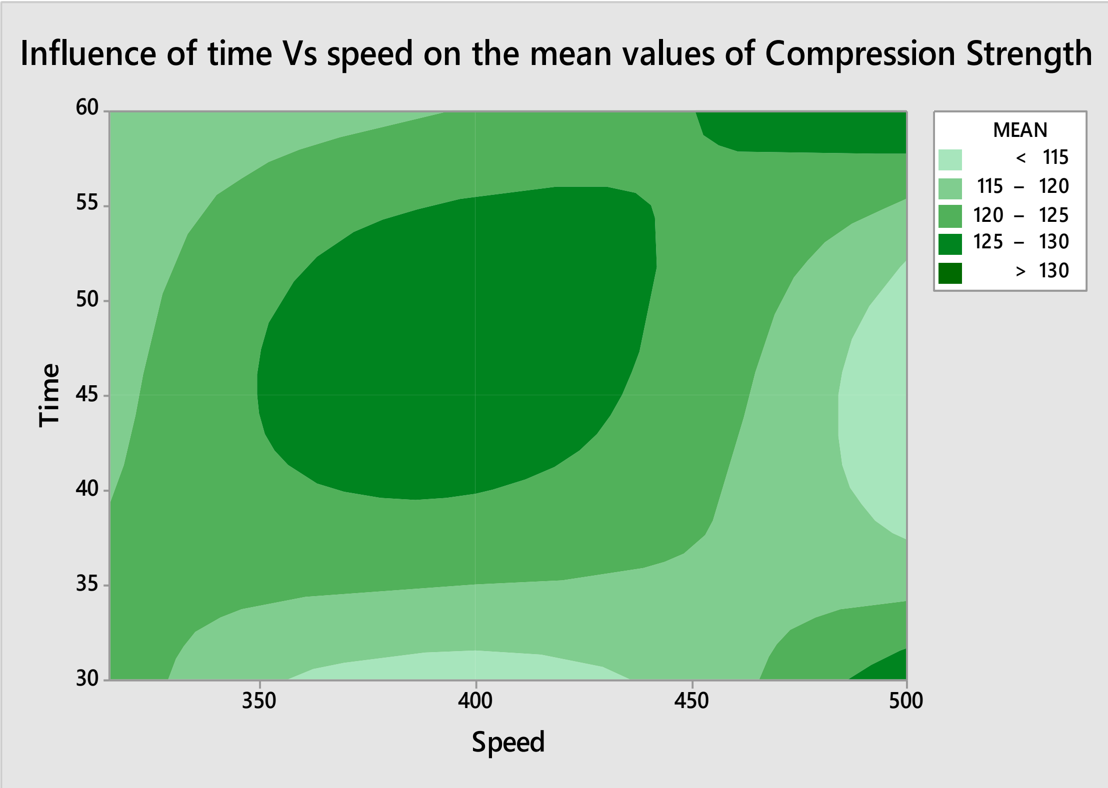

Figure 4. 11 Influence of time versus speed on the mean values of compression strength

4.11 Confirmation Experiment for Compression Strength

The final step of the DOE is the confirmation test, which verifies if the optimum conditions suggested by the matrix experiment do indeed give the improvement projected. The verification experiment is performed by conducting a test with optimal settings of the factors and levels previously evaluated by MINITAB 17. The confirmation experiments were conducted by adjusting the optimum set ups revealed by MINITAB 17 of Signal to noise ratios (i.e. 25.4/3 500Rpm 60s) in three trials to verify optimal friction stir consolidation process for compression strength response as shown in Figure 4.10. This combination is found in the seventh row of OA.

Table 4. 10 Verification experiment result on hardness response

Exp. No.	Speed (rpm)	Aspect ratio	Time (s)	E1	E2	E3
1	500	25.4/3	60	129.88	132.58	129.45

Verification experimentation result shows that mean is 130.64 and signal to noise ratio is calculated according to eq. (3.1) as:

$$\text{Mean} = \left(\frac{129.88+129.45+132.58}{3}\right) = \underline{130.64}$$

$$\text{S/N ratio } (\eta) = -10 \log_{10}\left(\frac{1}{n}\right)\sum_{i=1}^{n}\frac{1}{y_{ij}^{2}} \tag{3.4}$$

$$\text{S/N} = -10 \log_{10}\left(\frac{1}{3}\right)\left[\left(\frac{1}{129.88}\right)^2 + \left(\frac{1}{129.45}\right)^2 + \left(\frac{1}{132.58}\right)^2\right]$$

$$\text{S/N} = -10 \log_{10}[0.00017584704]$$

$$\text{S/N} = \underline{37.54865}$$

Generally, the optimum combinations of control factors for compression strength and hardness are describes in Table 4.11 below.

Table 4. 11 Optimum combination setups.

No.	**Responses**	**Optimum combination of control factor**
1	Compression strength	Speed 500 rpm, aspect ratio 25.4/3, 60 s
2	Hardness	Speed 500 rpm, aspect ratio 25.4/3, 60 s

4.12 Microstructural Analysis of Sample Produced by Optimum Setting

Generally compression strength and hardness of metals increase as the grain size decreases. The disc produced with optimum combination (25.4/3, 500 rpm and 60s) was cross-sectioned axially and radially in order to analyze its internal microstructure. The grain size of the axial cross-section is calculated as shown in APPENDIX B, and the result shows the average grain diameter for axial cross-section is 0.0124mm. The average grain diameter for cross section obtained as 0.0127mm. Therefore, the grain diameters of the disk is finer in its axial cross section as compared to its radial cross section.

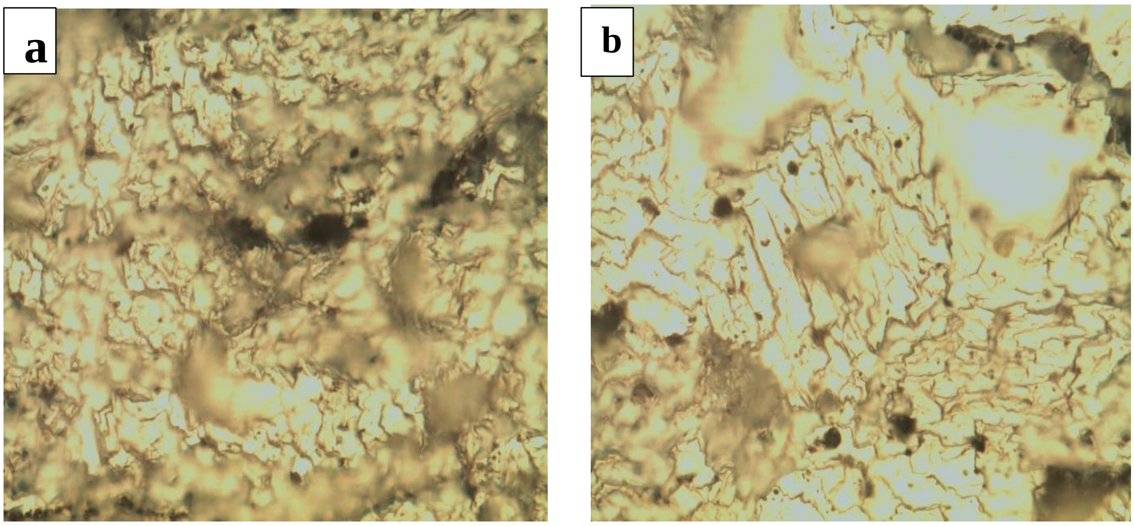

Figure 4. 12 Microstructural view of (a) axial and (b) cross-sectional of optimal sample

CHAPTER FIVE: CONCLUSION AND RECOMMENDATIONS

5.1 Conclusion

Discs from AA5052 was successfully fabricated through friction stir consolidation process. The obtained results of mechanical properties (hardness, compressive strength) and microstructural information are a clear evidence to conclude that AA5052 is consolidable under friction stir consolidation process. In addition to this, design of experiment was employed to determine the optimum processing set up to produce a sound disk with acceptable compression strength and hardness.

Based on post-analysis of experimental data, and consolidated discs, the following conclusions are drawn:

(1) The FSC process has two distinct stages: compaction and consolidation. In the compaction stage, the material is largely compacted but not well integrated. The voids between material particles are substantially reduced, approaching zero, but welding of the chips to each other does not occur. In the consolidation stage, material density increases slightly.

(2) With a combination of high temperature and severe plastic deformation, consolidation is formed at the top of chips charge as the process progresses. The fully consolidated region reach the high radial position at the bottom of the chamber after expanded processing time.

(3) The effects of die rotational speed, aspect ratio, and processing time on hardness and compression strength of disc have been analyzed via design of experiments. For the hardness response the effect of processing time and aspect ratio are higher as compared to die rotational speed. And for compression strength response aspect ratio and speed has higher influence.

(4) As the aspect ratio, consolidating time and die rotational speed increase the compression strength and hardness values were improved. In addition, the grain sizes also reduced which results in improvement of mechanical properties.

(5) The Minitab 17 analysis showed the percentage contribution of each factors for hardness response are concluded as Aspect ratio, Speed and Time with percentage contribution of 88.33%, 3.63% and 7.61% respectively with error percent of 0.43%.

(6) The effect of aspect ratio, speed and consolidation time on a compressive strength were determined and found as 77.69%, 5.32% and 4.27% respectively with error percent of 12.72%.

(7) Since the percentage contribution of the aspect ratio is high (88.33% and 77.69% for hardness and compression strength respectively) in comparison to the other two factors, therefore it is the most significant factor in FSC process.

(8) Finally the optimum set up of input factors with their respective levels are analyzed by Minitab 17 as: Aspect Ratio at level of 25.4/3, Speed at level of 500 Rpm, Time at level of 60s are the optimum set up for the improvement of compression strength and hardness of the AA5052 sample under FSC process.

5.2 Recommendations

Having passing through observation and experience, the researcher would like to recommend the following points. So that researchers can be able to extend their research areas on Friction stir consolidation processes.

1) Interested body can take temperature as one input factor and optimize FSC process. In order to quantify the temperature, infrared thermometer can be used to quantify the temperature inside the chamber.
2) It is better to use a split consolidation die for easy removal of the produced disc. In addition, under die design sample removing mechanism should be included if it is not possible to provide a split die.

5.3 Scope of Future Work

Depending on the FSCP understanding, methods employed and result analysis techniques used, the following is recommended as a future research work.

1) Optimization of process parameters of FSCP for AA5052 (by taking input factors: Load, Time, Temperature, Speed and Aspect ratio)
2) Establish FEA simulation to better predict and describe heat stress distribution inside the sample and dies.
3) FEA simulation assisted die design for FSC Process.
4) Using FSC process for composite material fabrication.

REFERENCES

- Andrews, D. R., & Gilpin, M. J. (1975). FRICTION FORGING-A PRELIMINARY STUDY. *Metall Mater Technol*, *7*(7), 335-357.
- Catalini, D., Kaoumi, D., Reynolds, A. P., & Grant, G. J. (2013). Friction Consolidation of MA956 powder. *Journal of Nuclear Materials*, *442*(1-3), S112-S118.
- Catalini, D., Kaoumi, D., Reynolds, A. P., & Grant, G. J. (2015). Dispersoid distribution and microstructure in Fe-Cr-Al ferritic oxide dispersion-strengthened alloy prepared by friction consolidation. *Metallurgical and Materials Transactions A*, *46*(10), 4730-4739.
- Cooper, D. R., & Allwood, J. M. (2014). The influence of deformation conditions in solid-state aluminium welding processes on the resulting weld strength. *Journal of Materials Processing Technology*, *214*(11), 2576-2592.

- Cooper, D. R., & Allwood, J. M. (2014). The influence of deformation conditions in solid-state aluminium welding processes on the resulting weld strength. *Journal of Materials Processing Technology*, *214*(11), 2576-2592.

- Duflou, J. R., Tekkaya, A. E., Haase, M., Welo, T., Vanmeensel, K., Kellens, K., ... & Paraskevas, D. (2015). Environmental assessment of solid state recycling routes for aluminium alloys: can solid state processes significantly reduce the environmental impact of aluminium recycling?. *CIRP Annals*, *64*(1), 37-40.

- Duflou, J. R., Tekkaya, A. E., Haase, M., Welo, T., Vanmeensel, K., Kellens, K., ... & Paraskevas, D. (2015). Environmental assessment of solid state recycling routes for aluminium alloys: can solid state processes significantly reduce the environmental impact of aluminium recycling?. *CIRP Annals*, *64*(1), 37-40.

- Galanty, M., Kazanowski, P., Kansuwan, P., & Misiolek, W. Z. (2002). Consolidation of metal powders during the extrusion process. *Journal of Materials Processing Technology*, *125*, 491-496.
- Gronostajski, J. Z., Kaczmar, J. W., Marciniak, H., & Matuszak, A. (1997). Direct recycling of aluminium chips into extruded products. *Journal of Materials Processing Technology*, *64*(1-3), 149-156.
- Gronostajski, J., & Matuszak, A. (1999). The recycling of metals by plastic deformation: an example of recycling of aluminium and its alloys chips. *Journal of Materials Processing Technology*, *92*, 35-41.

- Gronostajski, J., & Matuszak, A. (1999). The recycling of metals by plastic deformation: an example of recycling of aluminium and its alloys chips. *Journal of Materials Processing Technology*, *92*, 35-41.
- Gronostajski, J., & Matuszak, A. (1999). The recycling of metals by plastic deformation: an example of recycling of aluminium and its alloys chips. *Journal of Materials Processing Technology*, *92*, 35-41.

- Gronostajski, J., Marciniak, H., & Matuszak, A. (2000). New methods of aluminium and aluminium-alloy chips recycling. *Journal of materials processing technology*, *106*(1-3), 34-39.
- Güley, V., Güzel, A., Jäger, A., Khalifa, N. B., Tekkaya, A. E., & Misiolek, W. Z. (2013). Effect of die design on the welding quality during solid state recycling of AA6060 chips by hot extrusion. *Materials Science and Engineering: A*, *574*, 163-175.
- Haase, M., Khalifa, N. B., Tekkaya, A. E., & Misiolek, W. Z. (2012). Improving mechanical properties of chip-based aluminum extrudates by integrated extrusion and equal channel angular pressing (iECAP). *Materials Science and Engineering: A*, *539*, 194-204.
- Li, X., Baffari, D., & Reynolds, A. P. (2018). Friction stir consolidation of aluminum machining chips. *The International Journal of Advanced Manufacturing Technology*, *94*(5-8), 2031-2042.
- Li, X., Reynolds, A. P., Baoqiang, C., Jialuo, D., & Williams, S. (2015). Production and properties of a wire-arc additive manufacturing part made with friction extruded wire. In *TMS 2015 144th Annual Meeting & Exhibition* (pp. 445-452). Springer, Cham.
- Li, X., Tang, W., & Reynolds, A. P. (2012). Visualization of material flow in friction extrusion. In *ICAA13 Pittsburgh* (pp. 1659-1664). Springer, Cham.
- Li, X., Tang, W., & Reynolds, A. P. (2013). Material flow and texture in friction extruded wire. In *Friction Stir Welding and Processing VII* (pp. 339-347). Springer, Cham.
- Li, X., Tang, W., Reynolds, A. P., Tayon, W. A., & Brice, C. A. (2016). Strain and texture in friction extrusion of aluminum wire. *Journal of Materials Processing Technology*, *229*, 191-198.
- Max, S. (1945). *U.S. Patent No. 2,391,752*. Washington, DC: U.S. Patent and Trademark Office.

- Max, S. (1945). *U.S. Patent No. 2,391,752*. Washington, DC: U.S. Patent and Trademark Office.

- McDonald, D. T., Lui, E. W., Palanisamy, S., Dargusch, M. S., & Xia, K. (2014). Achieving superior strength and ductility in Ti-6Al-4V recycled from machining chips by equal channel angular pressing. *Metallurgical and Materials Transactions A*, *45*(9), 4089-4102.
- Misiolek, W. Z., Haase, M., Khalifa, N. B., Tekkaya, A. E., & Kleiner, M. (2012). High quality extrudates from aluminum chips by new billet compaction and deformation routes. *CIRP Annals-Manufacturing Technology*, *61*(1), 239-242.

- Misiolek, W. Z., Haase, M., Khalifa, N. B., Tekkaya, A. E., & Kleiner, M. (2012). High quality extrudates from aluminum chips by new billet compaction and deformation routes. *CIRP Annals-Manufacturing Technology*, *61*(1), 239-242.

- Oberg, E., Jones, F. D., Horton, H. L., Ryffel, H. H., & Geronimo, J. H. (2016). *Machinery's handbook* (pp. 1207-1209). Industrial Press, Incorporated.
- Paraskevas, D., Vanmeensel, K., Vleugels, J., Dewulf, W., Deng, Y., & Duflou, J. R. (2014). Spark plasma sintering as a solid-state recycling technique: the case of aluminum alloy scrap consolidation. *Materials*, *7*(8), 5664-5687.
- R. Sathiskumar, N. Murugan, I. DinaharanandS.J. Vijay (2013). Prediction of mechanical and wear properties of copper surface composites fabricated using friction stir processing.
- Ross, P. J., & Ross, P. J. (1988). *Taguchi techniques for quality engineering: loss function, orthogonal experiments, parameter and tolerance design* (No. TS156 R12). New York: McGraw-Hill.
- Samuel, M. (2003). A new technique for recycling aluminium scrap. *Journal of Materials Processing Technology*, *135*(1), 117-124.
- Shamsudin, S., Lajis, M. A., & Zhong, Z. W. (2016). Evolutionary in solid state recycling techniques of aluminium: a review. *Procedia CIRP*, *40*, 256-261.
- Sharma, C. S., Nakagawa, T., & Takenaka, N. (1977). Recent development in the recycling of machining swarfs by sintering and powder forging. *Ann Cirp*, *25*(1), 121-125.
- Shigley, J. E. (2011). *Shigley's mechanical engineering design*. Tata McGraw-Hill Education.
- Tang, W., & Reynolds, A. P. (2010). Production of wire via friction extrusion of aluminum alloy machining chips. *Journal of Materials Processing Technology*, *210*(15), 2231-2237.
- Tang, W., & Reynolds, A. P. (2011). Friction consolidation of aluminum chips. *Friction Stir Welding and Processing VI*, 289.
- Tekkaya AE, Schikorra M, Becker D, Biermann D, Hammer N, Pantke K. Hot profile extrusion of AA-6060 aluminum chips. Journal of Materials Processing Technology. 2009; 209:3343-50.
- Tekkaya, A. E., Schikorra, M., Becker, D., Biermann, D., Hammer, N., & Pantke, K. (2009). Hot profile extrusion of AA-6060 aluminum chips. *Journal of materials processing technology*, *209*(7), 3343-3350.

- Tekkaya, A. E., Schikorra, M., Becker, D., Biermann, D., Hammer, N., & Pantke, K. (2009). Hot profile extrusion of AA-6060 aluminum chips. *Journal of materials processing technology*, *209*(7), 3343-3350.
- Tekkaya, A. E., Schikorra, M., Becker, D., Biermann, D., Hammer, N., & Pantke, K. (2009). Hot profile extrusion of AA-6060 aluminum chips. *Journal of materials processing technology*, *209*(7), 3343-3350.

- Thomas, W. M., Nicholas, E. D., & Jones, S. B. (1993). Friction extrusion. *Metal Working, Google Patents https://www. google. com/patents/US5262123 Google Scholar*.
- Whalen, S., Jana, S., Catalini, D., Overman, N., & Sharp, J. (2016). Friction consolidation processing of N-type bismuth-telluride thermoelectric material. *Journal of Electronic Materials*, *45*(7), 3390-3399.
- Widerøe, F., & Welo, T. (2013). Using contrast material techniques to determine metal flow in screw extrusion of aluminium. *Journal of Materials Processing Technology*, *213*(7), 1007-1018.

- Widerøe, F., & Welo, T. (2013). Using contrast material techniques to determine metal flow in screw extrusion of aluminium. *Journal of Materials Processing Technology*, *213*(7), 1007-1018.

- Widerøe, F., Welo, T., & Vestøl, H. (2010). A new testing machine to determine the behaviour of aluminium granulate under combined pressure and shear. *International Journal of Material Forming*, *3*(1), 861-864.

APPENDIX A

Exploded View of Equipment and Bill of Material

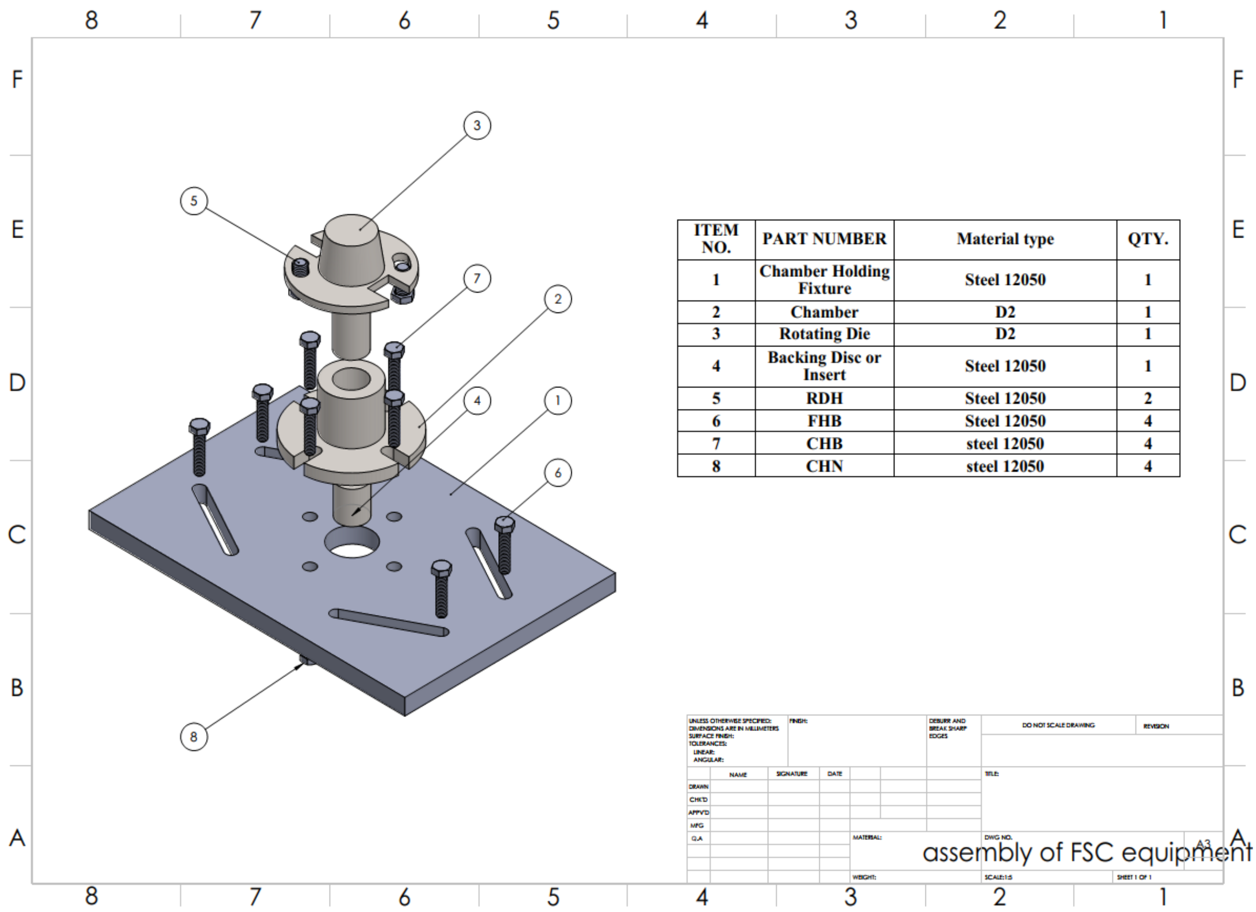

ITEM NO.	PART NUMBER	Material type	QTY.
1	Chamber Holding Fixture	Steel 12050	1
2	Chamber	D2	1
3	Rotating Die	D2	1
4	Backing Disc or Insert	Steel 12050	1
5	RDH	Steel 12050	2
6	FHB	Steel 12050	4
7	CHB	steel 12050	4
8	CHN	steel 12050	4

APPENDIX B

Calculations of Grain Sizes

According to ASTM E112-13 standard the average grain size is calculated as: Step in calculation of grain size

1) Determination of the magnification
2) Finding the grain size number
3) Solving for the average grain size diameter

1) Determine the magnification: in order to begin it is must to find the precise dimension of the photo.

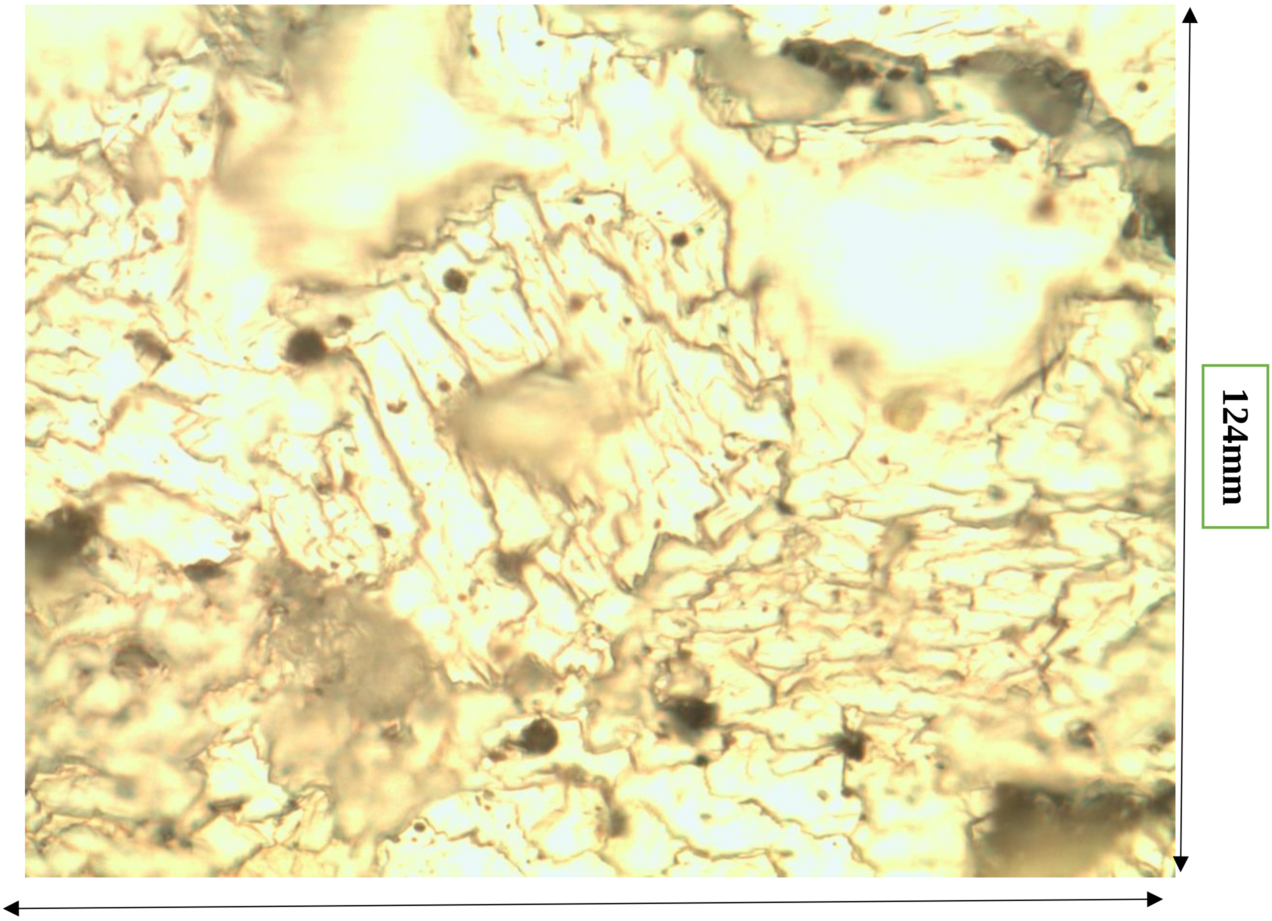

171 mm

It is possible to use the width or the height of the photo, and taking the width 171 mm then the actual width that the photo covers on the sample (i.e. AA5052) is 0.265 mm.

$$Magnification = \frac{Print\ width}{Real\ width}$$

$$Magnification = \frac{171\ mm}{0.265\ mm} = 645$$

2) Finding the grain size number.

Number of grains = whole grains + 0.5(partial grain)

This equation determines the number of grains in the given sample. Partial grains are found on the cut part the sample and full grain or whole grains or full grains are located inside the sample they are uncut grains. Therefore it is required to count the whole grains and partial grains to calculate the total number of grains in the picture.

Number of grain = 90 + 0.5(38) = 109

Since, it is already known the number of grains, it can be continued for solving grain size number.

True area = $\frac{W}{M} \times \frac{H}{M}$, where; W = width, H = height and M = magnification

$$\text{True area} = \frac{171\ mm}{645} \times \frac{124\ mm}{645} = 0.265 \times 0.192 = 0.0509\ mm^2$$

And this is the true area that the photo covers. And number of grain in this area is 109.

ASTM E112 relates grain size number with number of grains as follows:

$N = 2^{(n-1)}$ Where; n = grain size number, N = number of grain

So 1 inch 100 magnification photo is actually 0.254 mm on the specimen

$(1\ \text{inch})^2 = (0.254\ \text{mm})^2$, $1\ \text{in}^2 = 0.0645\ \text{mm}^2$, therefore the actual area for ASTM is 0.0645 mm^2

$N = 2^{(n-1)}$

N = (Number of grains) $\left(\frac{0.0645mm2}{True\ area}\right)$

N = (109) $\left(\frac{0.0645}{0.0509}\right)$ = 138.12, then in order to find the grain size number use the formula of

$N = 2^{(n-1)}$

Log (138.12) = (n-1) log (2)

$n = \left(\frac{\text{Log}(138.12)}{\text{Log}(2)}\right) + 1$

n = 8.133

3) Solving for average grain size diameter:

Average grain diameter = $\frac{Total\ true\ length}{Number\ of\ grains\ intercept}$

Total true length = $\frac{Length\ of\ line}{M} = \frac{2(124)}{645}$ = 0.384mm

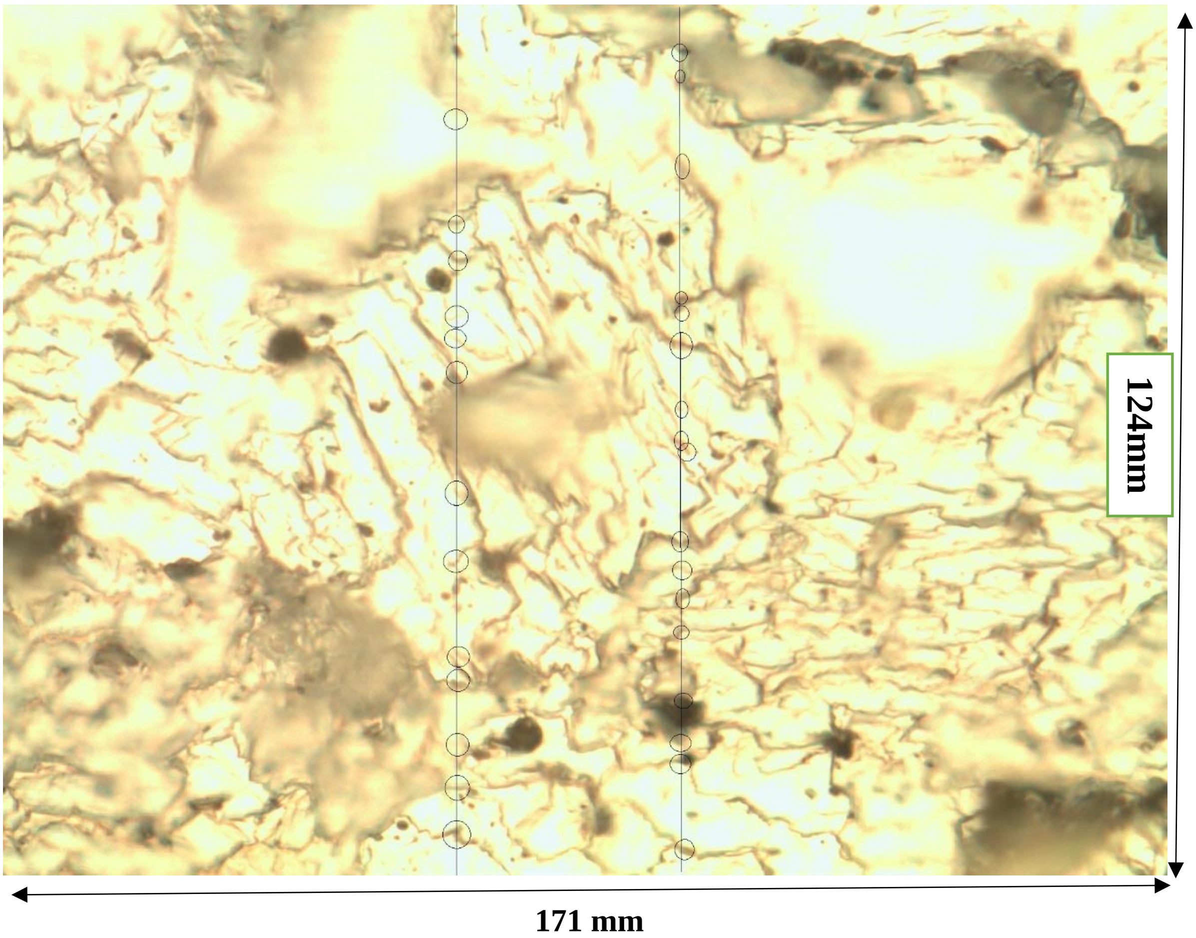

Then by counting number of grains intercepted on two vertical lines are = 13 + 18 = 31

Therefore; average grain diameter = $\frac{Total\ true\ length}{Number\ of\ grains\ intercepted} = \frac{0.384mm}{31}$

Average grain diameter = 0.0124mm

APPENDIX C

Microstructures with their combination set ups

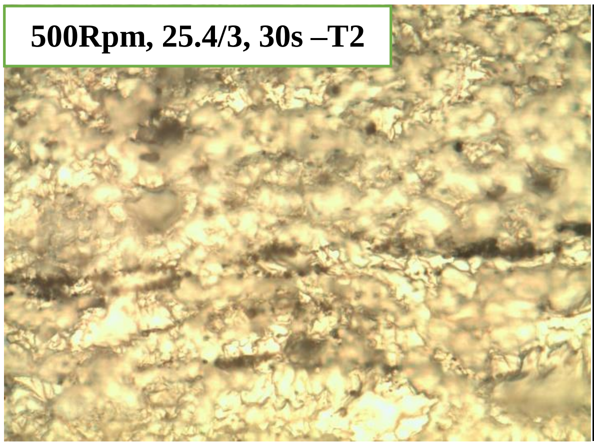

500Rpm, 25.4/3, 30s –T2

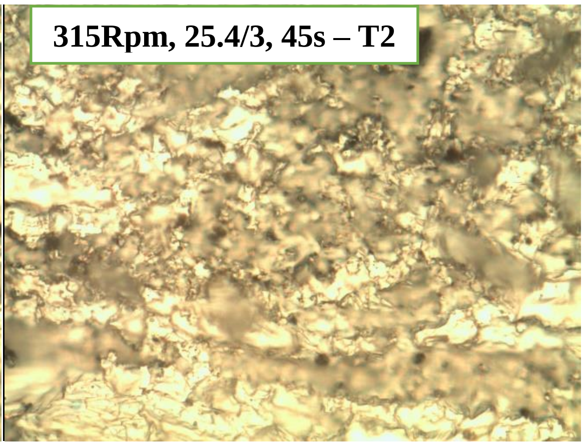

315Rpm, 25.4/3, 45s – T2

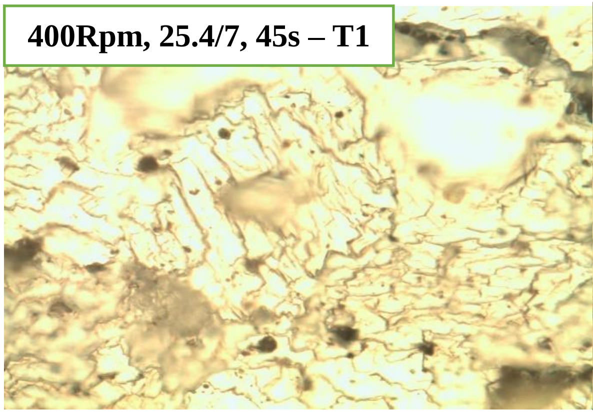

400Rpm, 25.4/7, 45s – T1

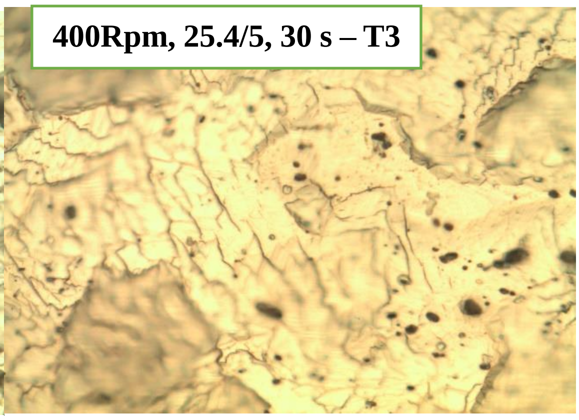

400Rpm, 25.4/5, 30 s – T3

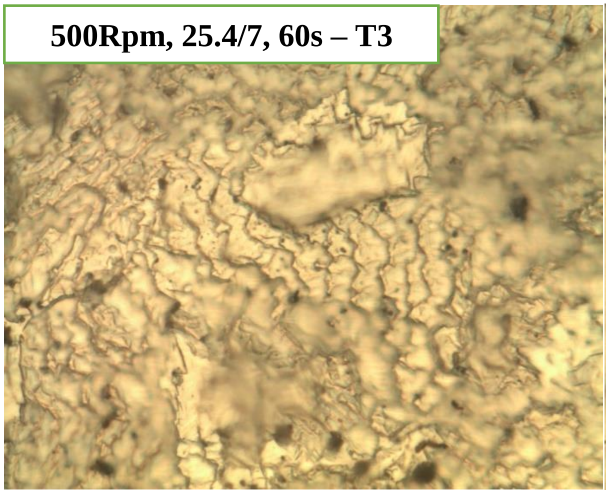

500Rpm, 25.4/7, 60s – T3

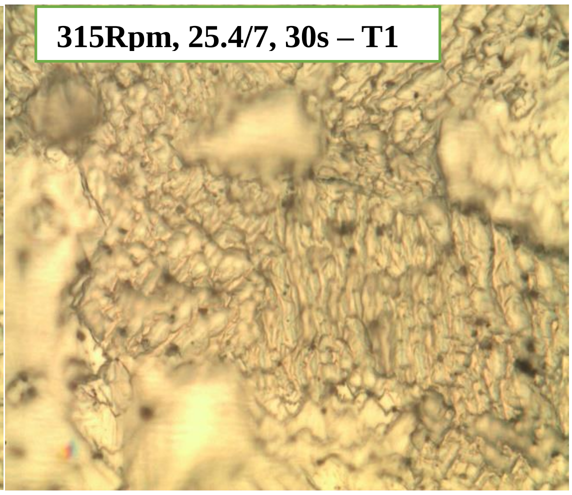

315Rpm, 25.4/7, 30s – T1

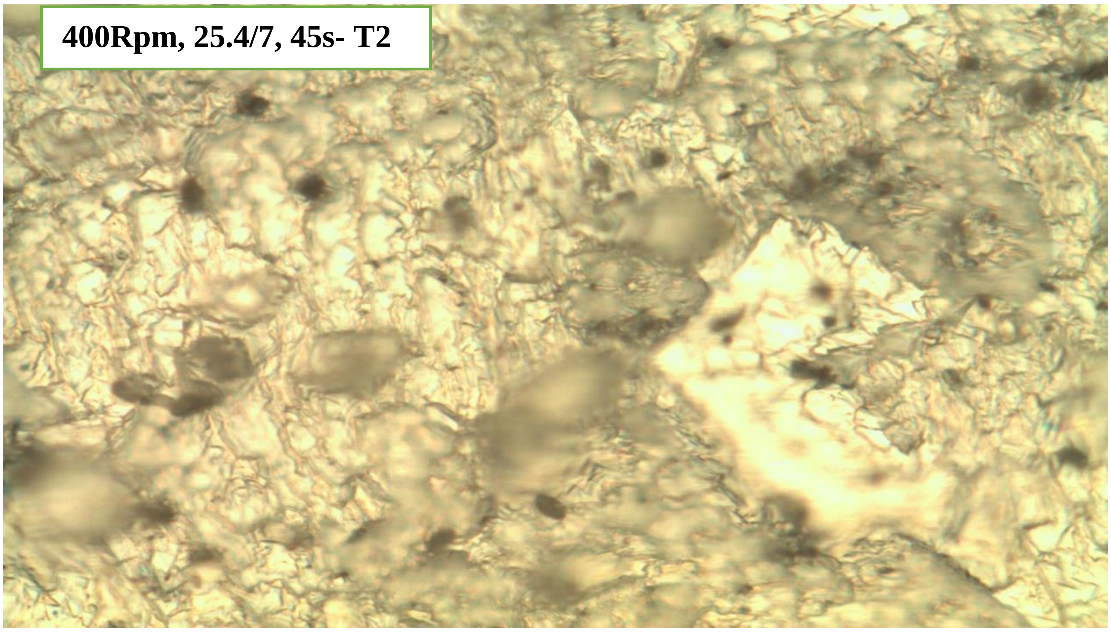

APPENDIX D

The hardness results

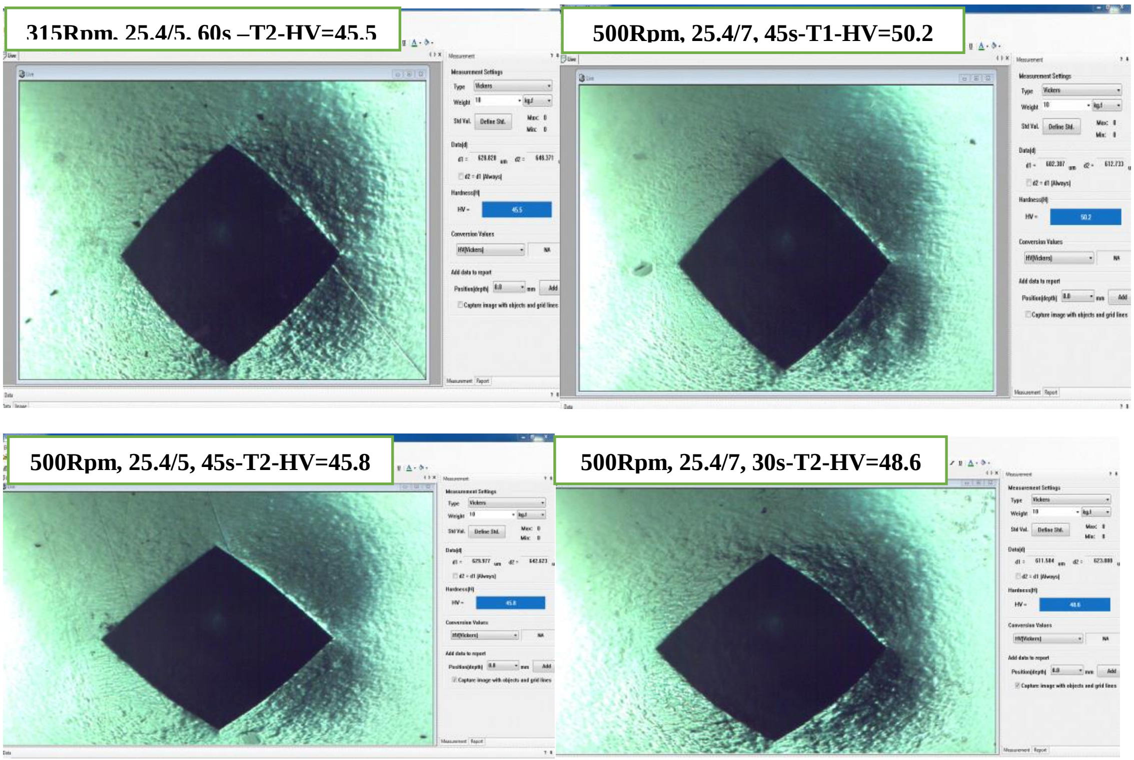

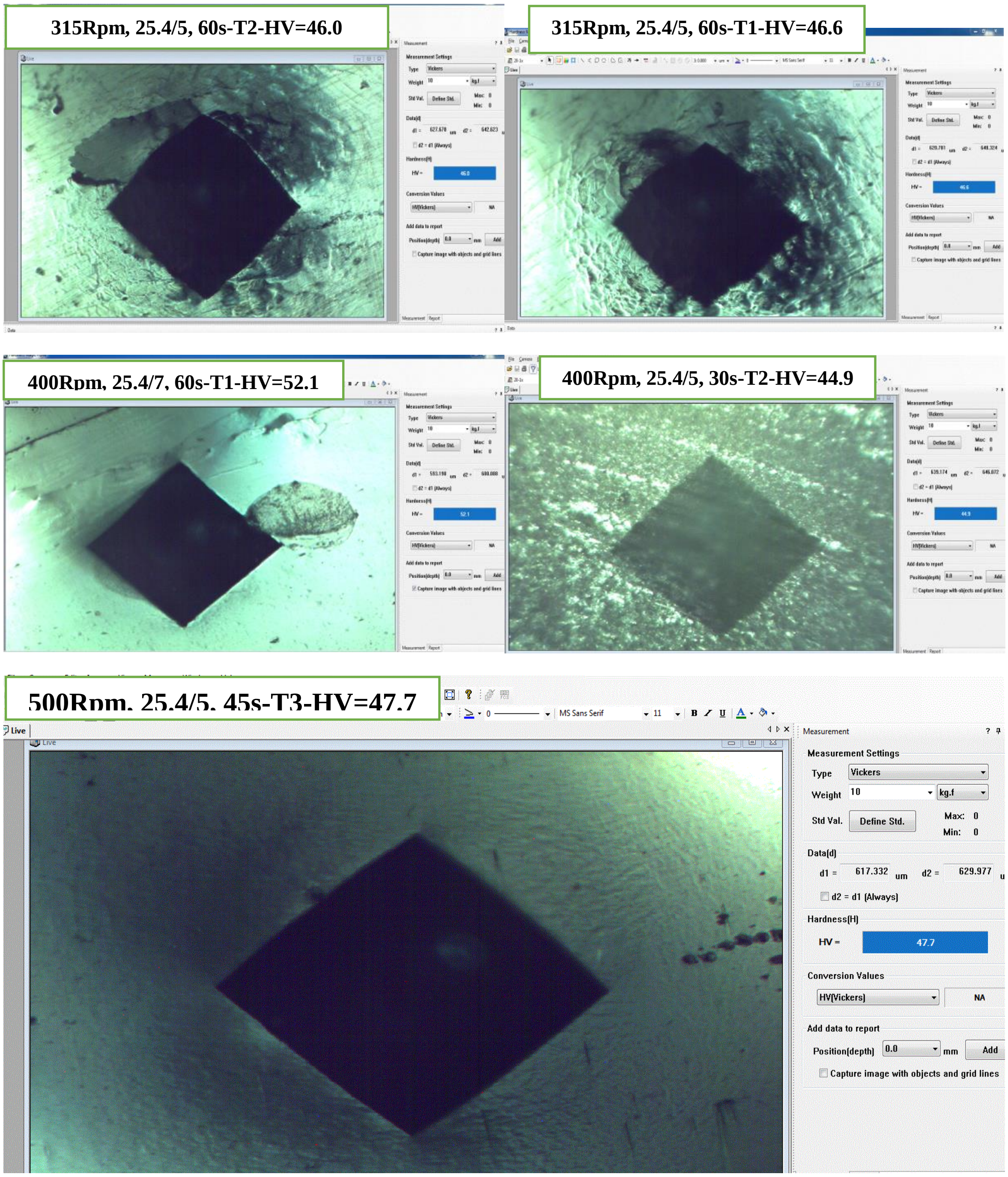
315Rpm, 25.4/5, 60s-T2-HV=46.0
315Rpm, 25.4/5, 60s-T1-HV=46.6
400Rpm, 25.4/7, 60s-T1-HV=52.1
400Rpm, 25.4/5, 30s-T2-HV=44.9
500Rpm, 25.4/5, 45s-T3-HV=47.7